Czech Technical University
Faculty of Nuclear Sciences and Physical Engineering
Department of Physics

Diploma Thesis

Analysis of RHIC results using SHARE and extending its capabilities to do fit of multiple datasets with shared parameters.

Bc. Michal Petráň

Supervisor: doc.RNDr.Vojtěch Petráček, CSc.
Prague, May 27, 2008

Contents

Abstract

Title:
Analysis of RHIC results using SHARE and extending its capabilities to do fit of multiple datasets with shared parameters.

Author: Michal Petráň

Specialization: Nuclear Engineering

Type of work: Diploma thesis

Supervisor: doc. RNDr. Vojtěch Petráček, CSc. Department of Physics, Faculty of Nuclear Sciences and Physical Engineering, Czech Technical University, Prague

Consultant: Dr.Prof. Johann Rafelski, University of Arizona

Abstract: My objective is to analyze the data from RHIC experiment for Au-Au collisions at $\sqrt{s_{\mathrm{NN}}} = 62.4\,GeV$ using the Statistical HAdronization with the REsonances (SHARE) program. The model parameters (temperature T, chemical potentials μ_B, μ_S, etc.) will be studied as a function of the number of participants A. Results of data analysis at 200 GeV show that some of the parameters are constant across centrality. For that reason, I plan to extend the SHARE program to be capable of fitting simultaneously several datasets with some of the parameters shared between them. This development will be tested by reviewing the analysis of Au-Au data at 200 GeV. The fit will have more degrees of freedom as some parameters are shared and new data for multistrange particles are available. This will solidify the results and get the start to centrality analysis as function of energy. In that way I hope to contribute to the understanding of dynamics of QGP expansion.

Key words: Quark-gluon plasma, Heavy-ion collisions, SHARE, statistical hadronization.

Abstrakt

Název práce:
Analýza výsledků experimentu RHIC za použití modelu SHARE a jeho rozšíření o možnost fitování více datových souborů se společnými parametry.

Autor: Michal Petráň

Obor: Jaderné inženýrství

Druh práce: Diplomová práce

Vedoucí práce: doc. RNDr. Vojtěch Petráček, CSc. Katedra fyziky, Fakulta jaderná a fyzikálně inženýrská, České vysoké učení technické v Praze

Konzultant: Dr.Prof. Johann Rafelski, University of Arizona

Abstrakt: Cílem této práce je nafitovat data z experimentu RHIC při srážkách Au–Au při energii $\sqrt{s} = 62.4\,GeV$ v programu Statistické HAdronizace s REzonancemi (SHARE). Parametry modelu (teplota T, chemický potenciál μ_B, μ_S, atd.) budou studovány v závislosti na počtu účastníků srážky A. Výsledky předešlých analýz při energii 200 GeV ukazují, že některé z parametrů modelu jsou konstantní pro všechny centrality. Z toho důvodu plánuji doplnit program SHARE o možnost simultáního fitování více vstupních datových souborů, které mají společný alespoň jeden parametr. Toto vylepšení bude otestováno na fitu srážek Au–Au při 200 GeV. Tento fit bude mít více stupňů volnosti, protože některé parametry budou společné a protože jsou k dispozici nová data pro "multistrange" částice. To potvrdí výsledky a umožní začít pracovat na závislosti na centralitě jako funkci energie. Takto, jak doufám, bych mohl přispět k pochopení dynamiky rozpínání kvark–gluonového plazmatu.

Klíčová slova: Kvark-gluonové plazma, Srážky těžkých iontů, SHARE, statistická hadronizace.

Prohlášení

Prohlašuji, že jsem svoji diplomovou práci vypracoval samostatně a použil jsem pouze podklady a zdroje (literatury, projekty, SW, atd.) uvedené v přiloženém seznamu.

Nemám žádný důvod proti užití tohoto školního díla ve smyslu §60 Zákona č. 121/2000 Sb., o právu autorském, o právech souvisejících s právem autorským a o změně některáých zákonů (autroský zákon).

V Praze dne: Podpis:

Acknowledgement

First of all, I would like to thank Dr.Prof. Johann Rafelski from the Univesity of Arizona for his invaluable help, motivation and guidance throughout the preparation of this work. Also I appreciate his time spent on reading through my work and language and factual corrections. I am grateful to doc.RNDr. Vojtěch Petráček, CSc. for his support during my studies at the Department of Physics of FNSPE.

I also express my gratitude to those, who gave me occasional, but very helpful, pieces of advice in different topics.

Finally, I am grateful to my parents for their patience and support during the whole time of my studies.

1 Introduction

What was the Universe like before $10\mu s$ after the Big Bang? Relatively small volume was occupied by very dense and very hot matter. Then the Universe expanded and cooled down until today state. Our aim is to simulate the initial very dense hot matter in a laboratory. We accelerate particles and nuclei up to high velocities and let them collide with each other. There are (for a very short period of time) similar conditions as in the early Universe.

We then concentrate on the study of the properties of this very dense hot phase of matter called Quark–Gluon Plasma (or QGP). It is supposed to contain unbound quarks and gluons existing together. We cannot observe this phenomenon elsewhere than in relativistic heavy–ion collisions. There are several experiments all around the world which contribute to this field; the heavy–ion program (SPS and upcoming LHC) at CERN, Geneva, Switzerland, or RHIC at BNL (USA). There is a variety of systems studied.

This is a vast field of physics with a lot of diverse activities, both experimental and theoretical. Let us concentrate in this thesis on one of the theoretical approaches to a description of heavy–ion collision, the statistical hadronization model (SHM). Then, let us have a look at some experimental results from Au–Au collisions at $\sqrt{s_{NN}} = 62.4\,GeV$ from RHIC and see how the model, implemented in the program SHARE, is in accordance with the results. This will help to understand how SHARE works and will help me upgrade it so it can fit multiple input files at the same time, so one can observe the dependance of the model parameters on different observables, such as the collision centrality (number of participants) or collision energy. It appears, that across centrality, the temperature is constant and therefore this fit will improve in quality, as one of the model parameters is shared among all the input files. Having this done, SHARE will be ready to be used to fit much more diverse tasks which are now impossible.

2 Statistical Hadronization Model

2.1 Statistics review

2.1.1 Classical approach

To describe in detail the properties of hot hadronic matter, we can use the approach of classical statistical physics (as can be found for example in [1], which I will briefly go through in the next few paragraphs. Then I will concentrate on the specific part of statistics needed to build up the statistical hadronization model (SHM).

Let us consider a large number N of identical coupled systems, which can be described by (for example) their energy E_i. Let us further assume, that these energies take only discrete values and that there are K macro states such that $K \ll N$. In other words, some of the energies E_i are occupied more then once, in general n_i times. Then we can write the total energy of the system as

$$E^{(N)} = \sum_{i=1}^{K} n_i E_i, \tag{2.1}$$

and it is conserved. From the definition immediately arises another condition:

$$\sum_{i}^{K} n_i = N. \tag{2.2}$$

Without any other quantum number (whose conservation we will introduce later), systems with the same energy E_i are indistinguishable from one another. The distribution $\boldsymbol{n} = \{n_i\}$ having the same energy E_i can be achieved in many different ways. To find out how many ways, let us consider the relation

$$K^N = (x_1 + x_2 + \cdots + x_K)^N|_{x_i=1} = \sum_{n} \frac{N!}{n_1! n_2! \cdots n_K!} x_1^{n_1} x_2^{n_2} \cdots x_K^{n_K}|_{x_i=1} \tag{2.3}$$

From there we can write the normalized coefficients

$$W(\boldsymbol{n}) = \frac{K^{-N} N!}{\prod_{i=1}^{K} n_i!}, \tag{2.4}$$

which have the meaning of relative probability of realizing each state in the ensemble $\boldsymbol{n}$ with n_i equivalent elements. To find the most probable distribution $\overline{\boldsymbol{n}}$ we can seek the maximum of the $\ln(W)$ from eq. (2.4). But we have to apply the constraints from eq. (2.1) and (2.2). We have a function A defined by

$$A(n_1, n_2, ..., n_K) = \ln W(\boldsymbol{n}) - \alpha \sum_i n_i - \beta \sum_i n_i E_i \tag{2.5}$$

with the constraints characterized by two Lagrange multipliers α and β. We seek its maximum the ordinary way, i.e. we find the partial derivative of A with respect to n_i:

$$\frac{\partial A}{\partial n_i} = \frac{\partial}{\partial n_i} \left(- \ln(n_i!) - \alpha n_i - \beta n_i E_i \right) |_{\overline{\boldsymbol{n}}_{max}} = 0 \tag{2.6}$$

Considering we have all $n_i \gg 1$, we can use the following formula for the derivative of the first term in eq. (2.6).

$$\frac{d}{dk}[\ln(k!)] \approx \frac{\ln(k!) - \ln[(k-1)!]}{k-(k-1)} = \ln k \tag{2.7}$$

Having this done gives us the well-known result of the most probable distribution $\overline{\boldsymbol{n}} = \{\overline{n}_i\}$, the exponential

$$\overline{n}_i = \gamma e^{-\beta E_i}, \tag{2.8}$$

where the inverse of the slope parameter β is the temperature T,

$$\beta = \frac{1}{T}, \tag{2.9}$$

and the quantity γ, which is seen in eq. (2.8) and which controls the total number of members of the ensemble N is the space occupancy.

$$\gamma \equiv e^{-\alpha} \tag{2.10}$$

Now, we can write again the total energy $E^{(N)}$ of the system employing the eq. (2.8) as follows

$$E^{(N)} = \sum_i \overline{n}_i E_i = \gamma \sum_i E_i e^{-\beta E_i}. \tag{2.11}$$

We can now express the number of ensemble members N in terms of the most probable distribution values as

$$N = \sum_i \overline{n}_i = \gamma \sum_i e^{-\beta E_i}. \tag{2.12}$$

When we want to know the average energy of each member of the ensemble N, we can express it as

$$\frac{E^{(N)}}{N} \equiv \overline{E^{(N)}} = \frac{\gamma \sum_i E_i e^{-\beta E_i}}{\gamma \sum_i e^{-\beta E_i}} \equiv -\frac{d}{d\beta} \ln Z. \tag{2.13}$$

Here we introduced the *canonical partition function* Z:

$$Z = \sum_i \gamma e^{-\beta E_i} \tag{2.14}$$

Now let us take into consideration another discrete observable that is equipartitioned as it is exchanged between macro systems apart from energy. In other words, we will work with the *grand-canonical ensemble*. We add a quantum number b, which can flow between the members of the statistical ensemble. For our convenience, let it be the baryon number, which is conserved in strong interactions. In analogy to the canonical ensemble formalism, we have the conservation of energy condition (eq. (2.1)) and the total number of members rests the same (eq. (2.2)) as well and we introduce another constraint for the baryon number conservation

$$\sum_{i=1}^{N} n_i^b b_i = b^{(N)} \equiv N\overline{b}_i, \tag{2.15}$$

where $b^{(N)}$ is the total baryon number of the ensemble and $\overline{b}_i$ is the average baryon number per member of the ensemble. The eq. (2.15) implicates another Lagrange multiplier in the function A (as in eq.(2.5)), whose maximum we will look for. For further convenience we write the third multiplier in the form $-\ln\lambda$. So we have

$$A(\boldsymbol{n}^b) = \ln W(\boldsymbol{n}^b) - \alpha \sum_i n_i^b - \beta \sum_i n_i^b E_i + \ln\lambda \sum_i n_i^b b_i \tag{2.16}$$

The derivative with respect to n_i^b, which we want to be zero at the maximum reads

$$\frac{\partial A}{\partial n_i^b} = \frac{\partial}{\partial n_i^b}\left[-\ln(n_i^b!) - n_i^b\alpha - \beta n_i^b E_i + \ln\lambda n_i^b b_i\right]\big|_{\overline{\boldsymbol{n}}_{max}} = 0 \tag{2.17}$$

The most probable distribution is then given by

$$\overline{n}_i^b = \gamma\lambda^{b_i} e^{-\beta E_i}. \tag{2.18}$$

The number of baryons in each ensemble is controlled by the *fugacity factor* λ and the factor γ (as introduced in eq. (2.11)). It is common to introduce the chemical potential μ as

$$\mu \equiv T\ln\lambda, \qquad\qquad \lambda = e^{\beta\mu} = e^{\mu/T}. \tag{2.19}$$

The chemical potentials have a physical meaning. They express the amount of energy necessary to add/remove a particle to/from the system at fixed pressure, energy and entropy.

Following the same method as before, we obtain for the average energy per particle

$$\overline{E^{(N)}} = \frac{\gamma\sum_{i;b} E_i\lambda^{b_i}e^{-\beta E_i}}{\gamma\sum_{i;b}\lambda^{b_i}e^{-\beta E_i}} \equiv -\frac{d}{d\beta}\ln\mathcal{Z}, \tag{2.20}$$

where we introduce $\mathcal{Z}$ as the *grand-canonical partition function.*

$$\mathcal{Z}(V,\beta,\lambda) = \gamma\sum_{i;b}\lambda^{b_i}e^{-\beta E_i} \tag{2.21}$$

$\mathcal{Z}$ can be seen also as the generating function for the canonical partition function Z_b

$$Z_b(V,\beta) = \frac{1}{2\pi i}\oint db\frac{1}{\lambda^{b+1}}\mathcal{Z}(\beta,\lambda), \tag{2.22}$$

where Z_b is a canonical partition function of a system with fixed baryon number b. The path of the integration in eq. (2.22) leads around the singularity at $\lambda = 0$. We can also express the average baryon number

$$\overline{b} = \frac{\sum_{i;b} b_i\lambda^{b_i}e^{-\beta E_i}}{\sum_{i;b}\lambda^{b_i}e^{-\beta E_i}} = \lambda\frac{d}{d\lambda}\left(\ln\sum_{i;b}\gamma\lambda^{b_i}e^{-\beta E_i}\right) \equiv \lambda\frac{d}{d\lambda}\ln\mathcal{Z}(\beta,\lambda) \tag{2.23}$$

2.1.2 Independent quantum (quasi-)particles

The discrete energies with which we worked above can be understood in the framework of quantum mechanics as the eigenenergies of the eigenstates $|i\rangle$ of a quantum Hamiltonian $\hat{H}$

$$\hat{H}\,|i\rangle = E_i\,|i\rangle \tag{2.24}$$

And since the operator $\hat{b}$ of the (conserved) baryon number commutes with the Hamiltonian, each state can be characterized by its baryon number (and/or other quantum number such as strangeness). So we have eq. (2.24) and

$$\hat{b}\,|i,b\rangle = b\,|i,b\rangle\,. \tag{2.25}$$

In this context we can rewrite the grand-canonical partition function from eq. (2.21) as

$$\mathcal{Z} = \sum_{i,b} \langle i,b|\,\gamma e^{-\beta(\hat{H}-\mu\hat{b})}\,|i,b\rangle = \mathrm{Tr}\,\gamma e^{-\beta(\hat{H}-\mu\hat{b})} \equiv \sum_n \langle n|\,e^{-\beta(\hat{H}-\mu\hat{b}-\beta^{-1}\ln\gamma)}\,|n\rangle\,. \tag{2.26}$$

This relation is very useful because the trace is independent of the representation. In other words, we can use any complete set of microscopic basis states $|n\rangle$ to find the (quantum) canonical or grand-canonical partition function. This allows one to obtain the physical properties of quantum gas in the approximation that it consists of practically independent particles and, eventually, we can incorporate any remaining interactions via perturbation expansion.

This approach can be used even for quasi-particles, which comprises a particle-like objects in a medium. They can have masses different from elementary particles, they can have masses induced by collective excitations. As long as we have well-defined excitations, it does not matter whether we work with real particles, or quasi-particles for the computation of the trace of the quantum partition function. By the use of quasi particles, we are including much of the effect of strong interaction between particles.
The occupation number is a suitable basis for the trace evaluation in (eq. (2.26)). Each macro state $|n\rangle$ is characterized by a set of occupation numbers $\boldsymbol{n} = \{n_i\}$ of the single (quasi-)particle states with baryon charge b_i of energy ε_i and the energy state is given by $E_n = \sum_i n_i\varepsilon_i$. The sum over all possible states correspond to the sum over all allowed sets $\boldsymbol{n}$: for fermions $n_i \in 0, 1$ and for bosons $n_i \in 0, 1, 2, \ldots, \infty$:

$$\mathcal{Z} = \sum_{\boldsymbol{n}} e^{-\sum_{i=1}^{\infty} n_i\beta(\varepsilon_i-\mu b_i-\beta^{-1}\ln\gamma)} = \sum_{\boldsymbol{n}}\prod_i e^{-n_i\beta(\varepsilon_i-\mu b_i-\beta^{-1}\ln\gamma)} \tag{2.27}$$

We can interchange the product and sum with the appropriate indices. We can do this since all the terms on the right hand side of eq. (2.28) is included on the right hand side.

$$\sum_{\boldsymbol{n}}\prod_i e^{-n_i\beta(\varepsilon_i-\mu b_i-\beta^{-1}\ln\gamma)} = \prod_i \sum_{n_i=0,1,\ldots} e^{-n_i\beta(\varepsilon_i-\mu b_i-\beta^{-1}\ln\gamma)} \tag{2.28}$$

Of course in the eq. (2.28) we sum over all allowed occupation numbers n_i, i.e $n_i = 0, 1$ for **F**ermions and $n_i = 0, 1, 2, \ldots$ for **B**osons. The resulting sums can be obtained analytically as:

$$\ln \mathcal{Z}_{F/B} = \ln \prod_i \left(1 \pm \gamma e^{-\beta(\varepsilon_i - \mu b_i)}\right)^{\pm 1} = \pm \sum_i \ln\left(1 \pm \gamma \lambda_i^b e^{-\beta \varepsilon_i}\right) \tag{2.29}$$

The plus sign applies to Fermions and the minus sigh applies to Bosons. Fermions have the Pauli occupancy $0, \gamma$ of each distinct single-particle state. Bosons on the other hand allows the occupancies $0, \gamma, 2\gamma^2, \ldots, \infty$. The factor γ^n arises naturally since we have not set the occupancy of each single-particle level to unity as is commonly done when absolute chemical equilibrium is assumed.
For antiparticles, the eigenvalues of $\hat{b}$ in eq. (2.29) are negative of those of particles values. Consequently, the fugacity $\lambda_{\overline{f}}$ for antiparticles $\overline{f}$ is

$$\lambda_{\overline{f}} = \lambda_f^{-1}. \tag{2.30}$$

Normally, this sign change is also introduced into the definition of chemical potential μ and we introduce chemical potential for antiparticle as

$$\mu_{\overline{f}} = -\mu_f \tag{2.31}$$

The energy of each (quasi-)particle is denoted by ε in eq. (2.29). For homogenous space-time, it is determined in terms of the mass m and the momentum $\vec{p}$ as

$$\varepsilon_i = \sqrt{m_i^2 + \vec{p}^2} \tag{2.32}$$

If energy is the only controlling factor, we carry out the level summation in terms of the single-particle level density $\sigma_1(\varepsilon, V)$:

$$\sum_i [\ldots] = \int d\varepsilon \, \sigma_1(\varepsilon, V)[\ldots] \tag{2.33}$$

To obtain σ_1, which we can understand as the number of energy levels in a box of volume $V = L^3$ per unit of energy ε, we note that quantum mechanics does not allow a continuous range of $\vec{p}$, as can be seen from eq. (2.32). Let us consider a box L^3 with periodic boundary conditions and we obtain a complete set of plane-wave states ψ, which meet the required periodicity.

$$\psi \propto e^{i(\vec{p}_\alpha \cdot \vec{X})} = e^{i\vec{p}_\alpha(\vec{X} + \vec{n}L)}, \tag{2.34}$$

where $\vec{n} = (n_1, n_2, n_3)$ with $n = 0, \pm 1, \pm 2, \ldots$. This fixes the allowed momentum values $\vec{p}_\alpha$ to

$$L\vec{p} \cdot \vec{n} = 2\pi k, \qquad k = 0, \pm 1, \pm 2, \ldots, \tag{2.35}$$

which can be satisfied only if

$$\vec{p}_\alpha = \frac{2\pi}{L}(k_1, k_2, k_3), \qquad \text{with } k_i = 0, \pm 1, \pm 2, \ldots. \tag{2.36}$$

Now the summation over all single-particle states is the same as the summation over all k_i. The number of permitted states equals the number of lattice points in the 'phase-space' k-lattice. In the limit of large L,

$$[\text{number of states in } d^3k] = \left(\frac{L}{2\pi}\right)^3 d^3p = \frac{V}{(2\pi)^3} d^3p \tag{2.37}$$

This way we have obtained the single-particle density σ_1 from eq. (2.33)

$$\sum_i [\ldots] = \int d\varepsilon \frac{V\, d^3p}{(2\pi)^3\, d\varepsilon} [\ldots] \tag{2.38}$$

We keep in mind that in general, whenever we replace a discrete-level sum with a limit of infinite volume of the system, it implies the phase-space integral

$$\sum_i \to g \int \frac{d^3x\, d^3p}{(2\pi)^3}. \tag{2.39}$$

Any other discrete quantum numbers such as spin, isospin, flavor, etc. contributes with an additive component of the same form in the sum of states and gives rise to the degeneracy factor g in eq. (2.39).

2.1.3 Quantum gases

When we have both particles and antiparticles, quantum–statistical grand canonical partition function eq. (2.29) for a particle of mass m and degeneracy g, we can write

$$\begin{aligned} \ln \mathcal{Z}_{F/B}(V,\beta,\lambda,\gamma) &= \pm gV \int \frac{d^3p}{(2\pi)^3} \Big[\ln(1 \pm \gamma\lambda e^{-\beta\sqrt{p^2+m^2}}) + \\ &\quad + \ln(1 \pm \gamma\lambda^{-1} e^{-\beta\sqrt{p^2+m^2}}\Big]. \end{aligned} \tag{2.40}$$

The second term in eq. (2.40) is due to antiparticles. When we do the expansion of the logarithms (assuming that the exponential term is small relative to unity), we get the classical Boltzmann limit:

$$\ln \mathcal{Z}_{cl}(V,\beta,\lambda,\gamma) = gV \int \frac{d^3p}{(2\pi)^3} \gamma(\lambda + \lambda^{-1}) e^{-\beta\sqrt{p^2+m^2}} \tag{2.41}$$

Often, the normalized particle spectrum is used. It is the average relative probability of finding a particle at the energy E_i, which is the coefficient of E_i in eq. (2.13), using eq. (2.8).

$$\begin{aligned} \overline{w}_i \equiv \frac{\overline{n}_i}{N} &= \frac{e^{-\beta E_i}}{\sum_j e^{-\beta E_j}} \\ &= -\frac{1}{\beta}\frac{\partial}{\partial E_i}\left(\ln \sum_j \gamma e^{-\beta E_j}\right) = -\frac{1}{\beta}\frac{\partial}{\partial E_i} \ln Z \end{aligned} \tag{2.42}$$

And now the single–particle spectrum can be evaluated. The particle distribution would then be

$$f_{F/B}(\varepsilon, \beta, \lambda, \gamma) = \frac{1}{\gamma^{-1}\lambda^{-1}e^{\beta\varepsilon} \pm 1}, \tag{2.43}$$

where the plus sign applies for Fermions and the minus sign for bosons. For antiparticles, the λ is replaced by λ^{-1}. In the classical limit the distribution reduces to

$$f_{F/B} \to f_{cl} = \gamma\lambda e^{-\beta\varepsilon} \tag{2.44}$$

2.2 Statistical hadronization

Now, the derivation of particle yields in the framework of SHM will follow. As eq. (2.43) states in agreement with [2], the entropy maximizing distribution can be written as

$$f_0(p^\mu, x) = \frac{1}{\gamma_q^{-1}\lambda_q^{-1}e^{u_\mu(x)p^\mu/T} + F} = \sum_{n=1}^{\infty} F^{n-1}\lambda_q^n e^{nu_\mu p^\mu/T}, \tag{2.45}$$

where the index q denotes, that we concentrate now on the light u, d quarks, p^μ is the four-momentum of the volume element under consideration, x its location in space and $u_\mu = \gamma(1, \vec{v})$ its four-velocity. The factor F is defined as

$$F = \begin{cases} -1 & \text{Fermions} \\ +1 & \text{Bosons} \\ 0 & \text{classical limit.} \end{cases} \tag{2.46}$$

If the interactions between particles will be strong enough that the mean free path is negligible with respect to the collective motion of the system, it will always have local thermal equilibrium and evolve as a continuous fluid and therefore the number current n^μ (for any conserved number such as baryon number, strangeness, isospin, etc.) and the energy tensor $T^{\mu\nu}$ will be conserved

$$\begin{aligned} \partial_\mu T^{\mu\nu} &= 0 \\ \partial_\mu n^\mu &= 0. \end{aligned} \tag{2.47}$$

As far as we can see, the Boltzmann formalism cannot be applied to the hadronization due to the phase transition from quark–gluon plasma to hadron gas, here 10 colored massless partons become over 200 'colorless' hadrons. But, according to lattice QCD calculations, the hadronization is a relatively fast process. In the rest–frame with respect to the collective flow, the hadrons will be distributed according to f_0 as given in eq. (2.45). The post hadronization current will be given by

$$j^\mu = \int d^3p \frac{p^\mu}{E} f_0(u_\mu p^\mu_{hadron}, T, \lambda_{hadron}) \tag{2.48}$$

We can then define a 'freeze-out hypersurface' defining a locus in space-time from which the statistically hadronizing particles are emitted. We can label the area by a four-vector Σ^μ. Since it is a 3-surface in a 4-space, it can be defined

as a function of three parameters (u, v, w). Then an element can be given in a Lorenz–covariant way using Stoke's theorem

$$d^3\Sigma_\mu = \epsilon_{\mu\nu\alpha\beta}\frac{\partial\Sigma^\nu}{\partial u}\frac{\partial\Sigma^\alpha}{\partial v}\frac{\partial\Sigma^\beta}{\partial w} \tag{2.49}$$

where $\epsilon_{\mu\nu\alpha\beta}$ is the Levi-Civita symbol. The number of particles produced in such a volume element is then Lorenz–invariant and computable in the volume element's rest frame as

$$j_\mu d^3\Sigma^\mu = dN \tag{2.50}$$

When we combine eq. (2.48) and (2.50), we obtain the famous Lorenz–invariant Cooper–Frye formula [4]

$$E\frac{dN}{d^3p} = \int d^3\Sigma_\mu p^\mu f(p_\mu u^\mu, T, \lambda) \tag{2.51}$$

Still, this formula do not take care of one situation. If the hadronization of the whole system takes a lot of time, the emitted particle can find itself in the QGP again if $p^\mu\Sigma_\mu < 0$. One option how to get rid of this is to truncate the distribution, to exclude this unphysical region from the integration. There is not a rigorous way at the moment how to solve this situation; however we can limit our calculation to only positive $\Sigma_\mu p^\mu$ by

$$E\frac{dN}{d^3p} = \int d^3\Sigma_\mu p^\mu f(p_\mu u^\mu, T, \lambda)\Theta(\Sigma_\mu p^\mu), \tag{2.52}$$

where $\Theta(x)$ is the step function. Now, let us think about hadron masses. All hadrons, except pions, have considerably higher mass, than the typical hadronization temperature ($p_\mu u^\mu > m \gg T$). Therefore the sum in eq. (2.45) can be truncated at $n = 0$, which correspond to the Boltzmann approximation

$$f(p_\mu) = \lambda e^{-p_\mu u^\mu/T} \tag{2.53}$$

When the thermodynamic parameters T, λ do not vary within the hadronizing volume, the total number of particles is independent of Σ^μ and u^μ. To see this, we can integrate the Cooper–Frye formula over momentum space

$$N = \int dN = \int \frac{d^3p}{E} p^\mu d^3\Sigma_\mu \lambda e^{p_\mu u^\mu/T}. \tag{2.54}$$

We can insert a unity $u_\mu u^\mu = 1$ in the integrand and we get

$$N = \left[\int d^3\Sigma_\mu u^\mu\right]\left[\int d^3p \frac{p^\mu u_\mu}{E} e^{p_\mu u^\mu/T}\right] \tag{2.55}$$

The first integral is just a normalization factor. Since $p^\mu u_\mu = E_{rest}$ the number of particles reduces to

$$N = Vg\int d^3p \lambda e^{-\sqrt{p^2+m^2}/T}, \tag{2.56}$$

where g is the degeneracy (for colorless particles, e.g. hadrons, it will be equal to $2S + 1$ where S is the spin). Using the Bessel function definition

$$K_n(x) = \frac{2^n n!}{(2n)!} x^{-n} \int_0^\infty \frac{dz}{\sqrt{z^2+x^2}} z^{2n} e^{-\sqrt{z^2+x^2}} \tag{2.57}$$

Having this done, we can finally find N analytically

$$N = g\frac{4\pi}{(2\pi)^3} m^2 \lambda T K_2\left(\frac{m}{T}\right) \tag{2.58}$$

Then the energy density in a rest frame with respect to the collective flow can be written as

$$\varepsilon = \int d^3\sqrt{p^2+m^2}\lambda e^{-\sqrt{p^2+m^2}/T} = g\frac{4\pi}{(2\pi)^3} m^3 \lambda T \left(\frac{3T}{m} K_2\left(\frac{m}{T}\right) + K_1\left(\frac{m}{T}\right)\right) \tag{2.59}$$

Looking back at eq. (2.45), the necessary changes to eq. (2.59) in order to generalize it to the Fermi–Dirac and Bose–Einstein distribution immediately follow.

$$\lambda T K_l\left(\frac{m}{T}\right) \to \sum_{n=1}^{\infty} (\pm 1)^{n+1} \frac{T}{n} \lambda^n K_l\left(\frac{nm}{T}\right) \tag{2.60}$$

If the particle has a finite width, the Bessel functions will be further integrated over the range of masses to take into account the mass spread. For a resonance with width, we obtain

$$N_i(m_i) \to \frac{1}{N_0} \sum_{\forall i\to j} \int_{m_{threshold}}^{\infty} n_i(M) F_\Gamma(M, \Gamma_i(b_{i\to j}, M)) dM \tag{2.61}$$

where

- $b_{i\to j}$ is the decay's branching ratio
- $m_{threshold}$ is the threshold mass for the decay, i.e. sum of masses of the products $\sum_j m_j$
- $F_\Gamma(M, \Gamma_i) = \frac{\Gamma\Gamma_i}{(M-m_i)^2+\Gamma_i^2/4}$ is the Breit-Wigner formula
- $\Gamma_i(b_{i\to j}, M)$ is the energy dependent width for decay under consideration. It can be non-trivial particle dependent function. To simplify the problem, we consider only the dominant energy dependence of the width, which means the decay threshold energy phase space factor. For the decays with low relative angular momentum, there has been an explicit form found to be

  $$\Gamma_i(b_{i\to j}, M) = b_{i\to j}\left[1 - \left(\frac{m_{threshold}}{m}\right)^2\right]^{l+\frac{1}{2}} \Gamma^* \tag{2.62}$$

  where l is the relative angular momentum of the decay and Γ^* is the energy independent constant found in the particle data book [3]

- N_0 is the Breit–Wigner and phase space normalization

$$N = \int_{m_{threshold}}^{\infty} F_{breit-wigner}(M, \Gamma_i(b_{i\to j}, M))dM = \\ = \int_{m_{threshold}}^{m_1} F_{breit-wigner}(M, \Gamma_i(b_{i\to j}, M))dM + \\ + \int_0^1 \frac{m_1 \Gamma_i\left(b_{i\to j}, \frac{m_1}{z}\right)}{(m_1 - m_i z)^2 + \frac{\Gamma^2\left(b_{i\to j}, \frac{m_1}{z}\right) z^2}{4}} dz, \tag{2.63}$$

  where the substitution $z = \frac{m_1}{m}$ is used in the last term.

2.2.1 Resonances decays

Most of the 200 hadrons produced in the statistical hadronization has a very short life-time, so they decay before they hit any detector. They cannot be reconstructed via the usual methods used for long-lived particles, they have to be reconstructed from their decay products, whose tracks are actually detected. There are also more complicated cascades of sequential decays of short-lived particles (for example $\eta' \to \eta\pi \to \pi\pi\pi\pi$ or $\Omega \to \Xi\pi \to \Lambda\pi\pi \to p^+ e^- \overline{\nu}_e \pi\pi$). Even though the number of particles coming from these decays is suppressed by high mass of the resonance, it is enhanced by the usually high spin degeneracy of the resonance and the fact that many particles are produced in a typical decay. For these reasons, the expected yields of light particles (such as pions or protons) will have to have the contribution from short-lived resonances decays included. Unfortunately there is no way to neglect their contribution to the particle yields (see fig. 2.1). On the other hand, in these decays, the quark (and therefore the baryon) number does not change in the decays, so their relative abundances are controlled by the temperature T only.

The resonances will be also a very sensitive probe of freeze–out. To include resonances in the particle yields and ratios, it is sufficient to add the decay products to the base particle yields

$$N_i \to N_i + \sum_{\forall j \to i + \ldots} b_{j\to i+\ldots} N_j, \tag{2.64}$$

where N_i is given particle yield as calculated from eq. (2.58) and $b_{j\to i+\ldots}$ is the branching ratio. There is one technical difficulty in this calculation. The decay products in particle data book [3] are presented, up to Clebsh-Gordan coefficient factor of isospin. In case of two–body decays, algorithms in CERNLIB can be (and in our calculations are) used

$$b_{j\to 12} = b^0_{0\to 12}(< J_0 m_0 | j_1 j_2 m_1 m_2 >)^2 \tag{2.65}$$

where $b^0_{0\to 12}$ denotes the branching ratio found in particle data book, J, m and j_i, m_i refers to the total and third isospin components of the resonance and products respectively.
For three–body decays we have to calculate the coefficients ourselves. There is several possible ways of combining partial isospin sums. We averaged over these

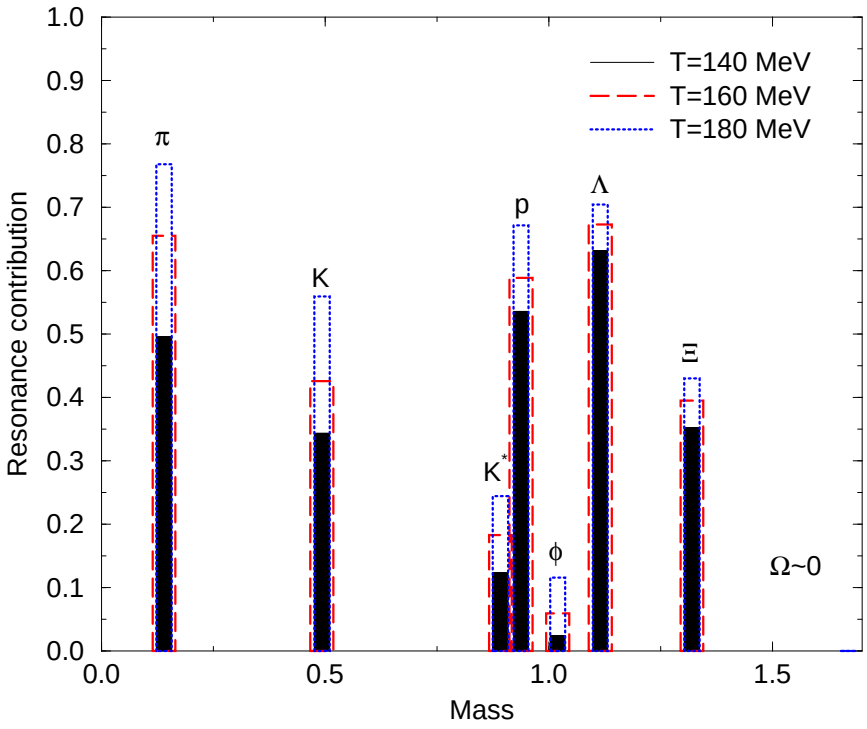

Figure 2.1: Resonance contribution to observed particle yields as a function of freeze-out temperature (taken from [2])

$$
\begin{aligned}
b_{j\to 123} &= b^0_{0\to 123}\frac{1}{3}[\sum_{j_{12}}(< J_{12}m_{12}|j_1j_2m_1m_2 >< J_0m_0|j_{12}j_3m_{12}m_3 >)^2 \\
&+ \sum_{j_{13}}(< J_{13}m_{13}|j_1j_3m_1m_3 >< J_0m_0|j_{13}j_2m_{13}m_2 >)^2 \\
&+ \sum_{j_{23}}(< J_{23}m_{23}|j_2j_3m_2m_3 >< J_0m_0|j_{23}j_1m_{23}m_1 >)^2] \qquad (2.66)
\end{aligned}
$$

The contribution of resonances to the particle spectra is non-trivial, since full kinematics has to be understood (for details see [2] for example). The resonance contribution to the particle spectra is where data is really sensitive to freeze–out dynamics because of post-hadronization processes can re-thermalize the decay products. Search for the resonance contribution reconstructed by the invariant mass is a good test of fast statistical freeze–out.
In analogy with eq. (2.64), we introduce

$$
E_1\frac{dN_1}{d^3p_1} = \left(E_1\frac{dN_1}{d^3p_1}\right)_{direct} + \sum_{\forall j\to 12..n}\left(E_1\frac{dN_1}{d^3p_1}\right)_{j\to 12..n} \qquad (2.67)
$$

where the first term is given by Cooper–Frye formula (eq. (2.52)) and the second gives the distribution of the decay products in a cascade. If j is also produced

by statistical hadronization, all we have to do is to find $E_1 \frac{dN_1}{d^3p_1}$ in terms of $E_j \frac{dN_j}{d^3p_j}$, which will be given again by the Cooper–Frye formula. These relations are recursive if j has a cascade component. So after a couple of steps, it will get to the calculation of heaviest resonance yield, which is calculated from the Cooper–Frye formula only.
Supposed that all the short-lived resonances have decayed and that there is a lot of particles produced in the hadronization and they are emitted in all directions, which means that all the matrix–elements are averaged over any dependence on factors such as spin. The distribution of the decay product momenta will then be given by the integral over the available region of the Lorentz–invariant phase space

$$\left(E_1 \frac{d^3N_1}{d^3p_1}\right)_{j\to 12..n} = B \int \frac{d^3p_j}{2E_j} \int T_n \left(E_j \frac{d^3N_j}{d^3p_j}\right) \tag{2.68}$$

where T_n is defined as

$$T_n = \prod_{i=2}^{n} \frac{d^3p_i}{2E_i} \delta(\sum_{i=2}^{N} p_i - p_1)\delta(\sum_{i=2}^{N} E_i - E_1 - E_j) \tag{2.69}$$

and B is a normalization factor to make sure that

$$\frac{N_{j\to 12..n}}{N_j} = b_{j\to 12..n} \tag{2.70}$$

2.2.2 Chemical parameters in statistical hadronization

As nicely summarized in [5], the effort of Dr. Rafelski and others lead to the development of SHARE (Statistical Hadronization with REsonances) suite of programs, which is capable (among others) of fitting chamical parameters (temperature T, chemical potential μ_B, etc.) to experimental data. It appears that the SHM describes well the overall particle yields. Due to large energy contents of the fireball, SHM uses the (grand–)canonical approach with a temperature–like parameter T (refered to as temperature further on). The SHM contains very little information about the nature of individual interactions, thus it embodies the principle of reaching simplicity in many–body dynamics, allowing to identify the interesting properties of the dense and hot primary matter formed in heavy–ion collisions.

Now, let us have a look at the formal description of the chemistery of QGP. The main objective is to understand how to describe the yields of the multitude of different hadrons emerging from the fireball. Each of the hadrons produced will have certain quantum numbers such as baryon number, strangeness, etc., which need to be followed and conserved in the reactions. There is a way to do this, we can characterize each hadron by its valence quark content and the related quantum numbers. Then, we can develop the relations between the valence quark count and hadron properties.
The yield of each particle is governed by global statistical parameters such as size of the system (volume V) and chemical freeze–out temperature T. Besides these, each particle's yield is further controlled by the particle fugacity, which

is obtained from two different chemical factors as we will introduce below (eq. 2.71),

$$\Upsilon_i \equiv \lambda_i^{\pm 1}\gamma_i = e^{\sigma_i^{\pm}/T}, \tag{2.71}$$

where $\sigma_i^{\pm}$ is the chemical potential of particle i (for anti–particles the minus sign applies). We see that for each particle and its anti–particle we have different fugacity Υ_i, or in other words, different chemical potential (from eq.2.71 $\sigma_i^{\pm} = T\ln\Upsilon_i$). We present different approach using λ_i and γ_i. It appears to be more convenient to control the difference and the sum of particles and anti–particles separately. Each of them is related to a different type of chemical equilibrium as seen in table 2.1.

Table 2.1: Chemical factors associated with different chemical equilibria (taken over from [5])

λ_i	controls 'nett', i.e. difference yield of quarks i and anti–quarks i	Relative chemical equilibrium
γ_i	controls overall abundance of quark i anti–quark i pairs	Absolute chemical equilibrium

Moreover, there is a difference in the dynamics of the reaction associated with these parameters, despite the fact that there is no difference in their function or their origin. To understand this, let us take an example of strangeness in the hadronic gas phase (see fig. 2.2). The two principle chemical processes are the redistribution of strangeness among particles, let them be Λ, π and N, K in this example, or the creation of strangeness.

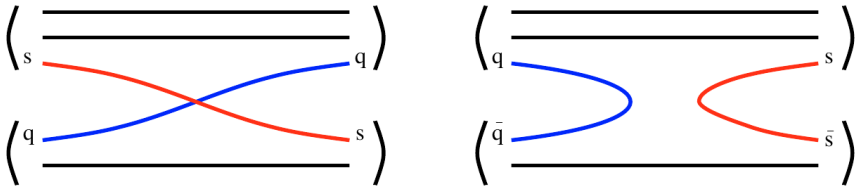

Figure 2.2: Typical strangeness exchange (left) and production (right) reactions in the hadronic gas phase (taken over from [5])

The left part of the figure 2.2 refers to a typical reaction of acquiring relative chemical equilibrium of the species involved via the exchange of strangeness. In this process, the quarks are not created, the available quarks are redistributed among thefinal hadrons. We can imagine the reaction $\Lambda + \pi \longrightarrow N + K$. On the other hand, we can have a reaction which will be responsible for the absolute chemical equilibrium of strangeness (right on the figure 2.2). In this case, the $s, \bar{s}$ pair is produced (and $q, \bar{q}$ annihilates). Reaching the absolute chemical equilibrium ($\gamma_s \to 1$) requires more rare collisions with annihilation and creation of quark pairs, such as $N + \pi \longrightarrow \Lambda + K$ in our example. However, these reactions are OZI suppressed (they have not connected diagram), which means that their cross sections are about a factor of $10 - 20$ weaker compared to the exchange

processes and thus they are slower in driving the absolute chemical equilibrium.

Now let us have a look how λ controls the difference between particle and anti–particle number and γ controls the yield of particle and anti–particle pairs. Assuming an example of a gas of nucleons and anti–nucleons $N, \bar{N}$. The two chemical fugacities will be:

$$\Upsilon_N = \gamma_N e^{\mu_N/T}, \qquad \Upsilon_{\bar{N}} = \gamma_N e^{-\mu_N/T}. \tag{2.72}$$

For the potentials it means

$$\sigma_N \equiv \mu_N + T\ln\gamma_N, \qquad \sigma_{\bar{N}} \equiv -\mu_N + T\ln\gamma_N \tag{2.73}$$

When we put this into the first law of thermodynamics, we get

$$\begin{aligned} dE + PdV - TdS &= \sigma_N dN + \sigma_{\bar{N}} d\bar{N} \\ &= \mu_N(dN - d\bar{N}) + T\ln\gamma_N(dN + d\bar{N}). \end{aligned} \tag{2.74}$$

From here, it is obvious, that the nucleon chemical potential μ_N controls the net nucleon number arising from the particle difference, while γ_N regulates the total number of nucleon and anti–nucleon pairs present. We call γ_N the phase space occupancy (of nucleons in this case).
In the the next example, we will develop this formalism for hadrons using the quark parameters. Let us take a gas of protons and anti–protons, whose valence quark content is as follows: $p(uud)$, $\bar{p}(\bar{u}\bar{u}\bar{d})$. We have:

$$\Upsilon_p = (\gamma_u^2\gamma_d)(\lambda_u^2\lambda_d) \qquad \Upsilon_{\bar{p}} = (\gamma_u^2\gamma_d)(\lambda_u^{-2}\lambda_d^{-1}) \tag{2.75}$$

Now we can rewrite the fugacities in terms of quark (and then baryon) chemical potentials:

$$\Upsilon_p = \gamma_u^2\gamma_d e^{\frac{2\mu_u+\mu_d}{T}} = \gamma_B e^{\frac{\mu_B}{T}} \qquad \Upsilon_{\bar{p}} = \gamma_u^2\gamma_d e^{\frac{-2\mu_u-\mu_d}{T}} = \gamma_B e^{\frac{-\mu_B}{T}} \tag{2.76}$$

Now we can add the third flavor of quark, the strange quark s. Let us describe the fugacity of $\Lambda(uds)$ and $\bar{\Lambda}(\bar{u}\bar{d}\bar{s})$ particles. We need to respect the negative S (strangeness) assignement to hadrons containing s quark, which could be comprised as a kind of anomaly in the formalism:

$$\Upsilon_\Lambda = \gamma_u\gamma_d\gamma_s e^{\frac{\mu_u+\mu_d+\mu_s}{T}} = \frac{\gamma_B}{\gamma_S} e^{\frac{\mu_B-\mu_S}{T}}, \quad \Upsilon_{\bar{\Lambda}} = \gamma_u\gamma_d\gamma_s e^{\frac{-\mu_u-\mu_d-\mu_s}{T}} = \frac{\gamma_B}{\gamma_S} e^{\frac{-\mu_B+\mu_S}{T}} \tag{2.77}$$

In order to focus on important parameters, we will introduce a little bit different formalism, which shows the good symmetry between u and d quarks and will simplify the notation as well.

$$\lambda_q \equiv \sqrt{\lambda_u\lambda_d}, \quad \mu_q \equiv \frac{\mu_u+\mu_d}{2}; \qquad \lambda_{I_3} \equiv \sqrt{\frac{\lambda_u}{\lambda_d}}, \quad \mu_{I_3} \equiv \frac{\mu_u-\mu_d}{2}. \tag{2.78}$$

and for the phase space occupancies

$$\gamma_q \equiv \sqrt{\gamma_u \gamma_d}; \qquad \gamma_{I_3} \equiv \sqrt{\frac{\gamma_u}{\gamma_d}} \tag{2.79}$$

Now we can summarize the formalism for nucleons generalized as $N(qqq)$, for single strange hyperons generically called $Y(qqs)$ and even double strange particles generically called $\Xi(qss)$:

$$\begin{aligned}
\Upsilon_N &= \gamma_q^3 e^{\frac{3\mu_q}{T}} = \gamma_B e^{\frac{\mu_B}{T}}, & \Upsilon_{\overline{N}} &= \gamma_q^3 e^{\frac{-3\mu_q}{T}} = \gamma_B e^{\frac{-\mu_B}{T}}, \\
\Upsilon_Y &= \gamma_q^2 \gamma_s e^{\frac{2\mu_q+\mu_s}{T}} = \frac{\gamma_B}{\gamma_S} e^{\frac{\mu_B-\mu_S}{T}}, & \Upsilon_{\overline{Y}} &= \gamma_q^2 \gamma_s e^{\frac{-2\mu_q-\mu_s}{T}} = \frac{\gamma_B}{\gamma_S} e^{\frac{-\mu_B+\mu_S}{T}}, \\
\Upsilon_\Xi &= \gamma_q \gamma_s^2 e^{\frac{\mu_q+2\mu_s}{T}} = \frac{\gamma_B}{\gamma_S^2} e^{\frac{\mu_B-2\mu_S}{T}}, & \Upsilon_{\overline{\Xi}} &= \gamma_q \gamma_s^2 e^{\frac{-\mu_q-2\mu_s}{T}} = \frac{\gamma_B}{\gamma_S^2} e^{\frac{-\mu_B+2\mu_S}{T}}.
\end{aligned} \tag{2.80}$$

We could write the formulas for $\Omega(sss)$ and $\overline{\Omega}(\bar{s}\bar{s}\bar{s})$, kaons and all other strange particles. There is another historical anomaly in the relations above, which is to be settled. To relate the quark and hadron quantum numbers, there is only one choice:

$$\mu_B = 3\mu_q,\ \mu_S = \mu_q - \mu_s; \qquad \mu_q = \frac{1}{3}\mu_B,\ \mu_s = \frac{1}{3}\mu_B - \mu_S. \tag{2.81}$$

These realtions in other words suggest, that there is no baryon number associated with strange quarks. Thus, even though strange quarks contain baryon number, if one respects the historical definitions, they are counted as baryon–free when it comes to hadronic chemistry. There is a simple way to check the published results without doing the re–computation. One can check the baryon anti–baryon ratios;

$$\left(\frac{\bar{\Lambda}}{\Lambda}\right) \Big/ \left(\frac{\bar{p}}{p}\right) = \left(\frac{\bar{\Xi}}{\Xi}\right) \Big/ \left(\frac{\bar{\Lambda}}{\Lambda}\right) = \left(\frac{\bar{\Omega}}{\Omega}\right) \Big/ \left(\frac{\bar{\Xi}}{\Xi}\right) = e^{+2\mu_S/T} \tag{2.82}$$

The above relations are held in most cases. There is only one special case which has to be taken care of, that is when there is a u/d quark asymmetry, that is to say λ_{I_3} different from unity. In this case one has to replace the ratios in the following manner:

$$\frac{\bar{p}}{p} \to \lambda_{I_3}^2 \frac{\bar{p}}{p}, \qquad \frac{\overline{\Xi}}{\Xi} \to \lambda_{I_3}^{-2} \frac{\overline{\Xi}^+}{\Xi^-} \tag{2.83}$$

2.2.3 Chemical (non–)equilibrium

As one can find for example in [9], the expanding fireball of QGP is not necessarily in chemical equilibrium. The statistical hadronization model parameters, which allows us to describe such eventuality are the γs introduced in section 2.2.2. Usually we define the degree of chemical equilibration for each flavor, i.e. light quark equilibrium by $\gamma_q^{EQ} = 1$, strange quark equilibrium by $\gamma_s^{EQ} = 1$, etc. In this work, we will not consider any heavier quarks in non-equilibrium, even though there is no particular reason to differentiate charm quark from strange quark. Note, that SHARE is ready for the study of charm (non–)equilibrium

with implemented γ_c parameter (see also section 3.2).

- The above mentioned chemical *equilibrium model* is defined by fixing the parameters $\gamma_q = 1$ and $\gamma_s = 1$. It further requires a complete chemical re–equilibration of all flavors after the hadronization (assuming that there was a complete equilibrium in the QGP phase) or, if there is no phase change, equilibration of all hadronic particles.

- The chemical *semi–equilibrium* model may arise from sufficiently slow hadronization, which gives enough time to the light quark abundances to re–equilibrate after hadron creation, but does not leave enough time for the strangeness to re–equilibrate, as it is considerably slower process. So the semi–equilibrium is described by $\gamma_q^{SE} = 1$ and $\gamma_s^{SE} \neq 1$.

- The chemical *non–equilibrium* of valence light and strange quarks assumes a rapid transformation of the deconfined quark–matter into free–streaming hadrons. In such sudden hadronization, there is not enough time to re–equilibrate the final state yields determined by the fragmentation and recombination of available QGP partons. Because the QGP phase has normally a different density than the hadron gas (HG) phase, the chemical equilibrium described by the quark–matter space occupancies ($\gamma_q^{QGP} = 1$, $\gamma_s^{QGP} = 1$) leads to chemical non–equilibrium in the immediately following HG phase and therefore the chemical non–equilibrium model is described by released parameters $\gamma_q^{NE} \neq 1,\ \gamma_s^{NE} \neq 1$.

Note that $\gamma_i > 1$ means extended yield of flavor i, there is more of the appropriate quarks than expected. On the other hand $\gamma_i < 1$ would describe a situation, when there is less quarks of flavor i than expected, i.e. the yields would be overestimated by the equilibrium model.

3 SHARE

3.1 Main purpose

The SHARE (Statistical HAdronization with REsonances) is a collection of programs designed for the statistical analysis of particle production in relativistic and ultrarelativistic heavy–ion collisions. With the input of statistical parameters, it generates particle yields and ratios. It includes all resonances and their cascade decays from the Particle Data Book (for example [3]). The crucial factor behind the success of the statistical model is the complete treatment of these resonances. An interface to fit parameters of the model to experimental results is also provided.

At first, SHARE was developed in two different ways, one program written in FORTRAN 77 and the second in a form of Mathematica notebook, in order to see, whether their results are the same given the same input file. Unfortunately, Mathematica proved to be very slow and therefore the development of the Mathematica version of SHARE was abandoned, despite the advantages of the graphical environment and versatility. On the other hand, the FORTRAN version is still being developed and upgraded because of its potential.

Several statistical models have been developed apart from SHARE (see [6] and references therein). They incorporates production of all hadrons and known resonances with their decay chains. The individual hadron yields are obtined by evaluating the available phase space size. This type of hadronization should be understood as a bottom line for particle production. There can be of course some other microscopic mechanisms responsible for particle production, which would be most clearly visible for non-abundant (heavy) resonances. The statistical models have one common feature, at some point the hadronic system freezes and the produced particles fill out the available phase space according to statistical distribution. After that no new particles are produced, only the short–lived resonances decay into more stable particles increasing significantly their yields. Moreover, the system expands in all directions, which is an important difference between heavy–ion and elementary particles collisions.

The statistical hadronization programs need a very detailed input of the hadronic spectra and the definitions of the subsequent decays of hadron resonances. Any causeless assumption can cause a difference of physical significance at the outcome of the analysis. It is hard to follow this, because some information is still not available for relevant resonances and has to be assumed based on the current knowledge of hadron structure, in particular the degeneracy and decay patterns.

We can imagine the fireball as a pot of hot guark–gluon 'soup', from which the hadrons evaporate with the abundance proportional to available phase space. The quark chemical equilibrium in the pot implies that the evaporated hadrons should be around (but not necessarily exactly at) their chemical equilibrium as well. In this approach, the hadrons evaporate from the surface of the fireball. If we consider the sudden hadronization of the fireball, the particle production does not happen only on the surface of the fireball. The whole fireball of QGP

breaks into small drops consisting of one or more elementary hadronic particle species. The statistical model also applies in case of slow hadronization, which comprises the assumption, that there is enough time diverse hadronic particles to be produced and destroyed during the chemical (re)equilibration.

3.2 SHARE version 1

As one can find in [6], the SHAREv1 was published in 2004. It is a program written in `FORTRAN77`, which uses three libraries (`CERNLIB, kernlib` and `mathlib`). Other than that, SHARE is system independent as well as hardware independent. It is sufficient to have a computer with `FORTRAN 77` compiler. SHARE was tested under several distributions of Linux (Red Hat, FEDORA, Ubuntu, SLC, etc.) with several different compilers (f77, g77). This was done also in order to prevent compiler based errors and to make sure, that SHARE will work for most users. The program package is distributed as gzipped tarball archive, which includes the source code, a script for compilation and an example analysis files (with data from AuAu collisions at $\sqrt{s_{NN}} = 200$ GeV from RHIC).

3.2.1 Method

The distributions of both stable particles and hadronic resonances at freeze–out are calculated via a series of Bessel functions using the CERN libraries (see also eq. 2.58 and 2.60). There is as well an option to include finite particle widths of the resonances. One has to bear in mind that it is computationally much more time–consuming. On the other hand, it is necessary to implement the esence of the strong interaction dynamics within the statistical hadronization picture. The inclusion of finite width has a considerable effect when modeling directly detectable short–lived resonances such as $\Lambda(1520)$, K^*, etc. The resonances decays are done by adding of the parent abundances to the daughter, normalized by the branching ratio of the decay channel. We have to implement also the weak decays, which needs a special treatment. The daughter particle acceptance factors are introduced for all strongly interacting decay products. There is an interface implemented for fitting experimental particle ratios of the statistical model parameters with help of MINUIT [8]. The χ^2 function is defined in the standard way. For an investigated quantity f and experimental error Δf, we define χ^2 as

$$\chi^2 = \frac{(f_{experiment} - f_{theory})^2}{(\Delta f_{statistical} + \Delta f_{systematic})^2} \tag{3.1}$$

and number of degrees of freedom as

$$N_{DoF} = N_{data\ points} - N_{free\ parameters} \tag{3.2}$$

We separate the statistical and systematical errors since the statistical error is purely random variable, while systematic error is not, so they are implemented as independent. Aside from χ^2 the program also calculates the statistical *significance*, which is defined as the probability that the fitted χ^2 arises at or above the value given by a "true" theory and statistical (Gaussian) experimental error. In case that the best fit has low statistical significance (significantly less than unity), the model under consideration is most likely inappropriate. In the limit of many degrees of freedom (N_{DoF}), the statistical significance function

depends on χ^2/N_{DoF} with 90% statistical significance at $\chi^2/N_{DoF} \sim 1$ and falling steeply at $\chi^2/N_{DoF} > 1$. However, the number of degrees of freedom in fits involving ratios is usually not sufficient to reach the asymptotic limit. Need to note, that the statistical significance depends strongly on χ^2 and N_{DoF} separately. If $N_{DoF} < 20$, than in order to have an acceptable statistical significance, it is necessary to have χ^2/N_{DoF} significantly less then unity.

Need to mention that the fit routine does not always find the true χ^2 minumum. Especially in multi-parameter fit with low number of degrees of freedom has generally a non–trivial structure in the parameter space. One can find secondary minima, valleys, saddle points, etc. In order to help user do this, features like χ^2 and significance profile and contour computation has been implemented. With this tool, one can effectively find the true minimum. Having this done, the user can do a particle-by-particle comparison of the model and experiment in the program's comprehensive output.

3.2.2 Implementation

To summarize what was written in previous sections, the statistical model we are concerned with, have implemented the following features

- Particle abundances at chemical freeze–out,
- Resonance decays.

The program calculates the individual particle densities from

$$\begin{aligned} n(m_i, g_i, T, \Upsilon_i) =\equiv n_i &= g_i \int \frac{d^3p}{(2\pi)^3} \frac{1}{\Upsilon_i^{-1} \exp \sqrt{p_i^2 + m_i^2}/T \pm 1} \\ &= \frac{g_i}{2\pi} \sum_{n=1}^{\infty} (\mp)^{n-1} \Upsilon_i^n \frac{T m_i^2}{n} K_2(\frac{n m_i}{T}) \end{aligned} \tag{3.3}$$

in accordance with eq. (2.60). The equation (3.3) expresses the momentum integrals in terms of modified Bessel function K_2. This form is practical for numerical calculations in FORTRAN and is used there. The series converges when $\Upsilon_i e^{-m_i/T} < 1$. For the parameter ranges of interest, the only particle that could cause the series to diverge would be pions. In eq. (3.3), the lower sign is for bosons, the upper sign applies for fermions. $g_i = (2J_i + 1)$ is the spin degeneracy factor as we distinguish all particles according to their electrical charge and mass. Index i labels the different particle species both stable and unstable.

As mentioned before, one can use to define fugacity $\lambda_{I_3}, \lambda_q, \lambda_s$ and in more general case even λ_c which stands for charm quark fugacity factor, and γ_q, γ_s and γ_c as the phase space occupancies.

Resonances are treated at first as if they were normal particles with a well defined mass. After the freeze–out all hadronic resonances decay rapidly augmenting the stable particles' abundances. Some of the heavier resonances decay in cascades, which are implemented in the algorithm, where all decays proceeds sequentially from the heaviest to the lightest particle species. Therefore, the light particles obtain contributions from these resonances, which have the form

$$n_1 = b_{2\to1} b_{3\to2} \dots b_{N\to N-1}\, n_N \tag{3.4}$$

where $b_{k\to k-1}$ is the branching ratio for the $k \to k-1$ decay with the appropriate Clebsh–Gordan coefficient, which accounts for the isospin symmetry in strong decays and allows us to treat separately different charged states of isospin multiplets of particles, such as nucleons, pions, kaons, etc. One can see that on an example of different Δ isospin states. They decay in the following way:

$$\begin{aligned}
\Delta^{++} &\longrightarrow \pi^+ + p^+ \\
\Delta^{+} &\longrightarrow \frac{1}{3}(\pi^+ + n^0) + \frac{2}{3}(\pi^0 + p^+) \\
\Delta^{0} &\longrightarrow \frac{1}{3}(\pi^- + p^+) + \frac{2}{3}(\pi^0 + n^0) \\
\Delta^{-} &\longrightarrow \pi^- + n^0
\end{aligned} \tag{3.5}$$

Here the branching ratio is one, but the Clebsch–Gordan coefficients introduce another factor which in two cases leads to an effective branching ratio of $\frac{1}{3}$ or $\frac{2}{3}$. For three–body decays, the Clebsch–Gordan coefficients are averaged in accordance with eq. (2.66). The resonances can have more than one decay channel. All decay channels with branching ratio less then 1% are not implemented in the calculation. There is another rule for inclusion of the decays according to whether the decay channel is *dominant, large, seen* or *possibly seen* in Particle Data Book [3]. If the channel is *dominant*, others are not implemented. If there is more than one decay channel with the same designation, they are taken as equivalent with a branching ratio $1/n$ where n is the number of different channels. Sometimes, the branching ratios are not given exactly, a range of acceptable values is given. Then, a mean value is taken. It could happen that the sum of branching ratios for one mother particle differs from unity. In this case, the branching ratios are normalized to 1. Weak decays are added separately by the user and are added to the particle ratios as feed-down correction. They are identified by breaking flavor or isospin conservation. On the other hand, electromagnetic decays like $\Sigma_0 \to \Lambda + \gamma$ are implemented as if they were hadronic in the contribution to the yield of Λ.

3.2.3 SHARE structure

SHARE is a modular program. Its basic structure is illustrated in fig. 3.1.
Five input files are needed for the program to run properly. They should contain model and experimental data. There is one calculational and fitting block, which is controlled by a set of instructions in one file (called `sharerun.data`). Each command will be executed independently from the others and generate a separate output to a file of its own.

Any user defined file name of the specified length can be used for all input except the master control file `sharerun.data`. The defaults are:

`thermo.data` (11 letter filename)
`particles.data` (14 letter filename)
`decays.data` (11 letter filename)
`totratios.data` (14 letter filename)
`ratioset.data` (13 letter filename)

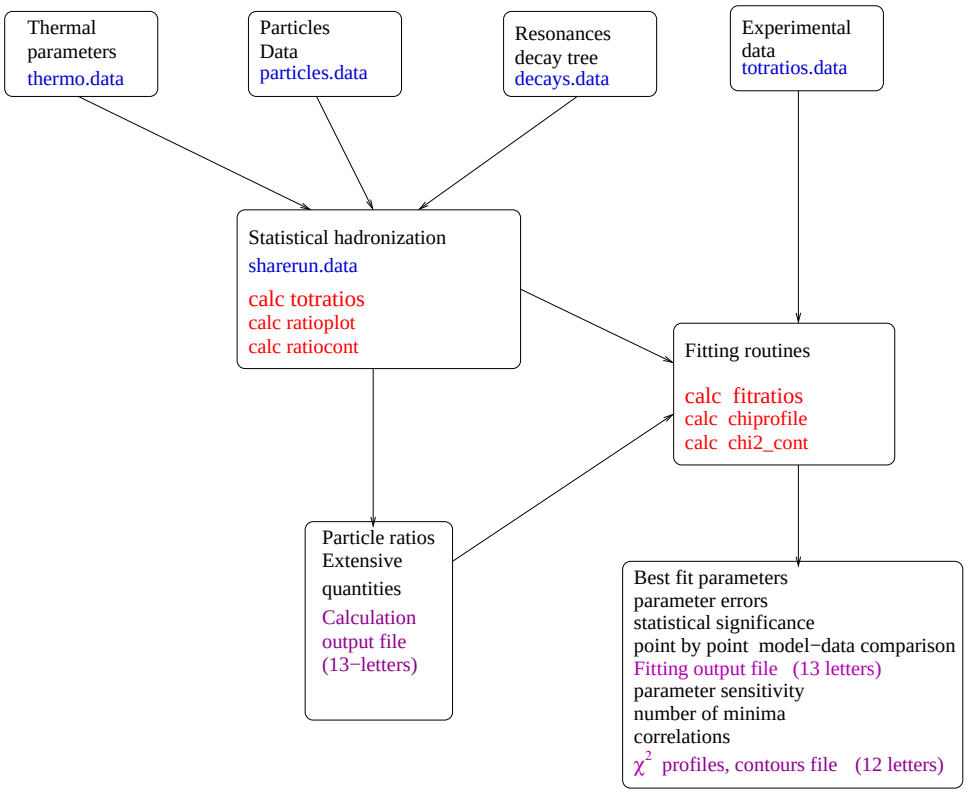

Figure 3.1: SHARE structure. Running commands which can be given are in red, default input filenames are in blue, while possible output files are in violet (color online). All output filenames are set by the user. (taken over from [6])

These input files include, respectively, initial thermal parameters defining the beginning of the fit procedure, particle properties, decay patterns, the experimental particle ratios and model parameters ranges. These input files are described in detail in the following paragraphs. It is possible to insert comments into all of these files: any time the first character starts with '#', the subsequent input line is disregarded.

Now let us have a look at each of the files' structure separately:

- **Thermal parameters' initial values file `thermo.data` (11 letter filename)**
  This file contains the initial values of the model parameters including temperature T and chemical potentials μ. The initial values of chemical potentials can be defined either directly with a value of μ_i, or more commonly by a value of γ_i (`gamq`, `gams` and `gamc`) and λ_i (`lamq`, `lams` and `lamc`). A description of an example `thermo.data` file with explanations is given in table 3.1. Where applicable, the units are GeV. Note that FORTRAN input must be formatted, so each thermodynamical parameter tag is a four–character string and between the tag and the appropriate value, there are two spaces needed. This applies also for the master control file

tag	value	explanation (not part of file)
temp	0.165	temperature
mu b	0.028	light quark fugacity or chemical potential
mu s	0.006	strange quark fugacity or chemical potential
gamq	1.	light quark phase space occupancy
gams	1.	strange quark phase space occupancy
lmi3	-0.001	I_3 fugacity or chemical potential
norm	1.	absolute normalization
lamc	1.	charm quark fugacity
gamc	0.001	charm quark phase space occupancy
accu	0.001	calculations accuracy

Table 3.1: Example of `thermo.data` file with brief parameter descriptions (taken over from [6])

`sharerun.data` (see next sections for details on the master control file).

- **Particle properties data file `particles.data` (14 letter filename)**
  This file contains information about particle properties such as mass, width, spin, isospin, quark content and the Monte Carlo identification code. The data is written in the following format:
  name mass width spin I $\mathbf{I_3}$ q s aq as c ac MC
  where:

name — a nine-letter character string identifying the particle,
mass — mass in GeV,
width — width in GeV,
spin — spin,
I — isospin,
$\mathbf{I_3}$ — 3rd component of isospin,
q, s — number of light/strange quarks,
aq, as — number of light/strange antiquarks,
c, ac — number of charm/anticharm quarks,
MC — particle's identification number, usually (where applicable) corresponding to the standard Monte-Carlo particle identification convention [3].

For example, the $\Delta(1232)^{++}$ will appear in the input file as

Dl1232plp 1.2320000 0.1200000 1.5 1.5 1.5 3 0 0 0 0 0 2224

As stated in [6], the quark number can have a non-integer value, to accommodate strong interaction flavor mixing such as that of the η. Note that SHARE calculations are relevant for a strongly interacting system, where the relevant states are K^0 and $\overline{K^0}$. $K^0 - \overline{K^0}$ mixing is an electroweak process occurring on a longer timescale, and therefore should be implemented at the end of the calculation as a weak feed-down.

In this file we use particle naming convention in the form of a 9-letter name through a letters-mass-ending combination (*e.g.,* Lm1115zer for

$\Lambda^0(1115)$), with the following usual three letter endings, which are given below:

zer for zero
zrb for zerobar
plu for plus
plb for plusbar
min for minus
mnb for minusbar
plp for plusplus
ppb for plusplusbar
sht for particle with this ending sht = $\frac{1}{\sqrt{2}}$ (zer+zrb)
e.g., K0492sht for $K_S = \frac{1}{\sqrt{2}}(K_0 + \overline{K_0})$
tot tot = (zer+zrb)
e.g., Lm1115tot for $\Lambda + \overline{\Lambda}$
mnt mnt = (min+mnb)
e.g., UM1321mnt for $\Omega + \overline{\Omega}$
pmb pmb = (plu+plb)
e.g., pr0938pmb for $p + \overline{p}$
plm plm = (plu+min)
e.g., Xi1321plm for $\Xi^+ + \Xi^-$

These conventions will be assumed also when fitting particle ratios and/or yields.

- **Particle decays pattern file `decays.data` (11 letter filename)**

This input file contains the information on particle decays. The data file lines are here written in the following format:

Name$_{\text{parent}}$ **Name**$_{\text{daughter1}}$ **Name**$_{\text{daughter2}}$ **Name**$_{\text{daughter3}}$[1] **BR C–G?(0/1)**

where **BR** refers to the branching ratio of this decay without the Clebsch–Gordan factor and C–G sets whether the branching ratio should be completed by the appropriate Clebsch–Gordan coefficient (0: no, 1: yes). For instance, the decays $\Delta^+ \to \pi^+ + n$ and $\Delta^+ \to \pi^0 + p$ will be given as (compare with eq. (3.5)):

```
Dl1232plu   pi0139plu   ne0939zer   1.0   1
Dl1232plu   pi0135zer   pr0938plu   1.0   1
```

while η decays will be:

```
eta547zer   gam000zer   gam000zer                0.3943   0
eta547zer   pi0135zer   pi0135zer   pi0135zer    0.3251   0
eta547zer   pi0139plu   pi0139min   pi0135zer    0.226    0
eta547zer   pi0139plu   pi0139min   gam000zer    0.0468   0
```

[1] In case of three–body decays

- **(Experimental) Values to be calculated (and fitted) `totratios.data` (14 letter filename)**
  Experimental data values of interest are submitted in in the following format.

  name1 name2 data random systematic fit?$(-1/0/1/2)$

  where

name1 The first particle in the ratio (numerator)
name2 The second particle in the ratio denominator. (Can also be a tag indicating the quantity is not a ratio but a yield or a density)
data The experimental value of the data point
random The random (statistical) error
systematic The systematic error
fit? This ratio contributes to the evaluation of χ^2/N_{DoF} if this parameter is set to 1 or 2. If the parameter is set to 0, the ratio is not fitted, but calculated and output to the graph file. If fit $= -1$ or 2 means the ratio is not output to the graph file.

  The entries in this files have a second use when name1 and name2 are not particle names but are as follows:

  In case **name2** is:

prt_yield the yield of the first particle or collective quantity.
prdensity the density of the first particle or collective quantity (in fm^{-3}).
solveXXXX See below.

  In case **name1** is:

negatives All negative particles stable under the strong interaction
totstrang strangeness[2] $\langle s \rangle$
netstrang net strangeness $\langle s - \bar{s} \rangle$
totenergy energy (in GeV)
totbaryon sum of all baryons and antibaryons, $B + \overline{B}$
netbaryon net baryon number, *i.e.,* baryons minus antibaryons, $B - \overline{B}$
totcharge charge Q
netcharge net charge $< Q - \overline{Q} >$
entropy_t entropy S

  A data file is provided as an example

```
#-----------------------------------------------------------
#------------  Extensive quantities (by Michal Petran)  -----
#-----------------------------------------------------------
weakdecay  WEAKnSTAR
#netstrang  solvelams     0.        0.         0.            0
tot_prime  prt_yield     0.        0.         0.           0
totstrong  prt_yield     0.        0.         0.           0
tot_multi  prt_yield     0.        0.         0.           0
```

[2]For this and the quantities below, volume normalization can be correct only when total particle yields are considered. The units of the calculated result vary according to whether the quantity is a density, a yield or a ratio.

```
totenergy  totstrong     0.        0.          0.           0
totenergy  tot_prime     0.98      0.01        0.           0
netstrang  totstrang     0.        0.05        0.           2
netcharge  netbaryon     0.39      0.01        0.           2
#--
#-------------------------------------------------------------
#---------------  Particle Yields (by Michal Petran)  -------
#-------------------------------------------------------------
pi0139min  prt_yield     237.      27.       0.           1
pi0139plu  prt_yield     233.      26.       0.           1
Ka0492plu  prt_yield     38.0     4.3        3.8          1
Ka0492min  prt_yield     32.6     3.7        3.2          1
Lm1115zer  prt_yield     13.88    0.23       1.39         1
Lm1115zrb  prt_yield     7.25     0.13       0.725        1
Xi1321min  prt_yield     1.84     0.11       0.18         1
Xi1321mnb  prt_yield     1.16     0.08       0.11         1
UM1672min  prt_yield     0.229    0.05       0.023        1
UM1672mnb  prt_yield     0.176    0.02       0.017        1
pr0938plu  prt_yield     34.3     3.8        3.43         0
pr0938plb  prt_yield     13.8     1.6        1.38         0
#---------------- other particles ----------------------------
pi0135zer  prt_yield     0.00      0.00        0.           0
Ka0492sht  prt_yield     0.00      0.00        0.           0
ph1020zer  prt_yield     0.00      0.0         0.           0
#------------------- RESONANCES ----------------------------
Ka0892sht  prt_yield     0.00      0.00        0.           0
Ka0892zer  prt_yield     0.00      0.00        0.           0
Ka0892zrb  prt_yield     0.00      0.00        0.           0
Dl1232zer  prt_yield     0.00      0.00        0.           0
Dl1232plp  prt_yield     0.00      0.00        0.           0
Lm1520zer  prt_yield     0.00      0.00        0.           0
Sg1385min  prt_yield     0.00      0.00        0.           0
Sg1385plu  prt_yield     0.00      0.00        0.           0
Lm1115zer  pr0938plu     0.65      0.          0.           0
Sg1189min  pr0938plu     0.3       0.          0.           0
#-------------------- Extensive quantities ------------------
totenergy  netbaryon     0.        0.          0.           0
stranghad  netbaryon     0.        0.          0.           0
entropy_t  netbaryon     0.        0.          0.           0
stranghad  entropy_t     0.        0.          0.           0
totenergy  T_entropy     1.02      0.015       0.           0
totenergy  entropy_t     0.        0.          0.           0
totenergy  stranghad     0.        0.          0.           0
totbaryon  negatives     0         0           0.           0
netbaryon  totbaryon     0.        0.          0.           0
pressuret  totenergy     0.        0.          0.           0
```

Figure 3.2: A typical input file with experimental data and wanted output

For the weak decay feed–down implementation and format in SHARE version 1 see [6]. It has been replaced by another format in the next version of SHARE (version 2), therefore it will be decsribed in detail for the up–to–date version in the next section (section 3.3).

- **Fit parameters `ratioset.data` (13 letter filename)**

The `ratioset.data` file contains the definition the parameters, which will be varied during the fit or kept constant. It further defines the range, in which the parameters will be varied, via the lower and upper limit of the particular parameter (for the use of MINUIT). It also sets the initial step size. The typical format is:

tag	lower / upper limit	step size	fit? (0/1)
temp	0. 1.	0.01	1
lamq	0. 10.	0.1	1
lams	0. 10.	0.1	1
gamq	0. 10.	0.01	1
gams	0. 10.	0.1	1
mui3	0. 10.	0.2	1
norm	0. 10000.	0.3	0
lamc	0. 10.	0.1	0
gamc	0. 10.	0.1	0

If the lower and upper limit are equal, MINUIT will fit with no limits, which is according to [8] more convenient, since the MINUIT converts the problem with defined limits to a problem with no limits via a non–linear transformation, which could make the initial problem more computationaly complicated. As stated in [8]; "it would transform a nice linear problem into a nasty non–linear one". On the other hand, by defining parameter limits, we can specify the physically interesting region and eliminate non–physical minima of χ^2.

If the only fit parameters are particle ratios and densities, the normalization is automatically kept fixed. The parameters can be input in any order. We have found that the fit quality (speed, reliability) depends considerably on the order of parameter input which is retained calling the MINUIT package: firstly, the most significant fit parameters should be input first (`temp, norm`). Secondly, the highly correlated parameters should be placed next to each other.

Note that values of parameters also arise as result of conservation laws rather than from fits to particle yields. For example, λ_s can be computed in terms of the other parameters requiring overall strangeness conservation within the phase space domain covered by the results considered. λ_{I_3} is similarly determined via the participant matter proton–neutron ratio, however, here it is possible to use this only when the data is available in 4π acceptance, since other hadrons can buffer the balance of charge condition. For example, at RHIC in the central rapidity region the large number

of pions implies in effect nearly symmetric $\lambda_{I_3} = 1$. Also, μ_B can be fixed through the participant number in the phase space region observed. The next section describes how SHARE allows the user to implement conservation laws either by solving the constraints (numerically) or by a fit.

Conservation laws

SHARE allows the user to solve for a fit parameter, rather than to find its value through a fit. For example, it is possible to implement strangeness conservation by numerical solution of the constraint equation

$$\langle s - \overline{s} \rangle = 0 \tag{3.6}$$

for λ_s. In this case, λ_s is not taken as a fit parameter anymore, but is understood as an analytical function of the other fit parameters and experimental particle yields.

To solve for a fit parameter, **name2** in the `totratios.data` file should be of the form **solveXXXX** where XXXX corresponds to the parameter 4-letter tag for which one wants to solve the equation. The parameter limits are still used by the program, as a constraint, solution outside the limits is rejected. This is useful for rejecting non–physical solutions of the constraint equation, such as $\lambda_s < 0$.

It is, in principle, possible to solve any data point for any thermal parameter. However, many such combinations do not have minima to which the equations converge nicely. If this is the case with a lot of MINUIT iterations, the minimization procedure can have difficulties to find the minimum.

It is therefore recommended that the solving algorithm is used only to solve for chemical potentials from conservation laws. For instance, to ensure strangeness conservation through solving the equation for λ_s the input file should contain the following line:
netstrang solvelams 0. 0. 0. 0. 0. 0
A line solving for λ_q from baryon conservation in case of Pb–Pb collisions might be
netbaryon solvelamq 362. 0. 0. 0. 0. 0
and the corresponding charge conservation statement will be
netcharge solvelmi3 142. 0. 0. 0. 0. 0
Note that it is also possible to implement conservation laws in terms of particle ratios. The two lines
netbaryon solvenorm 362. 0. 0. 0. 0. 0
netcharge solvelamq 142. 0. 0. 0. 0. 0
will fix λ_q in terms of the baryon/charge ($\frac{B}{Q} = \frac{p+n}{p} = 0.44$ for Pb-Pb) ratio even when the absolute normalization **norm** is a dummy variable which appears in no other data point and is not used in the fit.

The alternative to exact solving is to implement a conservation law by treating it as a data point. A line such as
netbaryon prt_yield 362. 10. 0. 0. 0. 1
will make sure that the baryon number is close to the one expected for Pb-Pb collisions at SPS. Similarly,

netstrang totstrang 0. 0.01 0. 0. 0. 1
will make conserve strangeness to one unit in 100 $s\overline{s}$ pairs, rather than solving the constraint exactly.

The choice of whether to implement the conservation law analytically or through a fit is therefore left to the user. It was found that both approaches are giving very similar results. However for an exact conservation law the most reliable approach is to use the exact constraint (analytical equation solution) only.

solve statements should be put at the top of the experimental ratios file. If this is not done, the program returns with an error.

Running the program, `sharerun.data` commands

This file contains the instructions which the program executes subsequently on running. Each line corresponds to a different operation, such as reading data files, assigning values to parameters, calculating ratios, minimizing and plotting contours and χ^2/N_{DoF} profiles. The program will read this file line by line, execute each command, and stop when it reaches the end of the file. Here is an example of a typical sharerun.data file.[3]

```
#
#---------- no width (file partnowdt.data),
#                    should not take that long
#
READ  PARTICLES  partnowdt.data  decays.data
#READ  PARTICLES  particles.data  decays.data
READ  TOTALDATA  totr00-05.data
#
#  Temperature initialization file (CAN ALSO USE PSET,
#                                   as in width calculation)
READ  THERM_INI  thermo.data
#
READ  FIT_PARAM  ratioset.data
#
# ---------  changes made by Michal Petran below
#
PSET  norm  900.
PSET  temp  0.1423
PSET  lamq  1.16
PSET  lams  1.056
PSET  gamq  1.0
PSET  gams  1.0
#PSET  mu_b  0.599
#
PFIX  gamq
PFIX  gams
CALC  FITRATIOS  fit_00-05.out
```

[3]The program, being written in FORTRAN, is very sensitive to the file's format. An extra space may cause the sharerun.data file (and other files as well) to be unreadable. Hence, it is recommended that the user bases his modifications on the sharerun.data (and other original files provided in the package) file shown in the fig. 3.3

```
#
#CALC  FITRATIOS  fit_00-05.Lmb
#CALC  CHIPROFIL  prf_gq_00-05  gamq  1.2  1.8  12
#CALC  SIGPROFIL  prof_G_00-05  gamq  0.2  1.6  40
#
PSET  norm  850.
READ  TOTALDATA  totr00-10.data
#CALC  SIGPROFIL  prof_G_00-10  gamq  0.2  1.8  40
CALC  FITRATIOS  fit_00-10.out
#
```

Figure 3.3: A typical sharerun.data file as I used

Each command can be used more than once for a fit with different options and input and output files, one at a time. Further on, a detailed description of each command's meaning and syntax is given. Keep in mind that 2 spaces have to be maintained between each word or number. The lines have the general form:

PSET <4-letter tag> VALUE
This Parameter SET command sets the thermodynamic variable defined by the TAG (name) to its designated VALUE. The initial command shown in figure 3.3, READ THERM_INI, comprises a series of PSET-type commands which read from an input file, covering all allowed thermal parameters.

READ THERM_INI <11-letter filename>
Reads the file corresponding to `thermo.data`, containing the initial values for the thermal parameters, as described above.

READ PARTICLES <14-letter filename> <11-letter filename>
Reads the file containing particle properties as well as the file containing the decay tree, as described in previous paragraphs

READ TOTALDATA <14-letter filename>
Reads the file containing experimental data and particle ratios to calculate, as described earlier.

PFIX tag FIXes the given thermodynamic Parameter to its current value. In a fit, that parameter will not be a variable.

PREL tag <Lower limit> <Upper limit> <Step size> RELeases the given thermodynamic Parameter, giving the limits and initial step size used in the fit.

READ FIT_PARAM <14-letter filename>
Reads the file containing fit parameters. It can be understood as a series of PFIX and PREL instructions read from an input file.

CALC RATIODATA <13-letter filename>
Calculates the value of the ratios read with the READ RATIODATA command and the current value of the thermal parameters (obtained either from READ THERM_INI or a previous fit). The output of the calculation is stored with the given filename, as a table in the following format:
RATIO NAM1/NAM2 <numerical value>

CALC RATIOPLOT Datapoint <12-letter Filename> tag L H P

Calculates the ratio of 2 particles, or a particle's yield, or a thermodynamic quantity, as a function of the variable represented by the 4-letter tag, in a parameter segment delimited by the limits (**L,H**) and number of points (**P**). The ratio to be calculated must be in the experimental ratios datafile; datapoint specifies which point to graph (for instance, if datapoint is 2, the second point from the top will be calculated). The output is saved as a 2-column table in the given output file, and can be plotted with packages such as PAW, Mongo, Xmgrace or GNUPlot.

CALC RATIOCONT datapoint <12-letter Filename>
tag1 L1 H1 P1 tag2 L2 H2 P2[4]

Calculates the ratio of 2 particles, or a particle's yield or density, or a thermodynamic quantity, as a function of two thermodynamic variables represented by the two 4-letter tags, in the parameter region delimited by the limits (**L1,2 H1,2**) and number of points. (**P1,2**. Note that an 100×100 grid has 10 000 points, and can take a long time to calculate). The ratio to be calculated is indicated in the same way as in **CALC RATIOPLOT**. The output is saved as a 3-column table in the given output file, and can be plotted with a program capable of 3D plots.

CALC FITRATIOS <13-letter filename>

Minimizes the χ^2/N_{DoF} of the set of experimental data obtained through READ RATIODATA according to the parameters in READ FIT_PARAM and initial values in READ THERM_INI. The output is written out to the given filename in the following format:

First, the output parameters (+/− error if fitted).

Then the detailed fit results, as a table with the format:

TOP BOTTOM THEORY EXPERIMENT TOT. ERROR. CHITERM

Where TOP and BOTTOM refer to each ratio's numerator and denominator, and CHITERM for each ratio refers to χ as defined in eq. 3.7

$$\chi = \frac{f_{\text{experiment}} - f_{\text{theory}}}{\Delta f_{\text{statistical}} + \Delta f_{\text{systematic}}} (= 0 \text{ if not fitted}) \tag{3.7}$$

Finally, the total $\chi^2/\mathrm{N_{DoF}}$ and fit statistical significance is presented. A typical output file is shown in figure 3.4

```
MINIMIZATION BEGINNING:
DATE: (YR MO DAY):  80417 TIME (HR MIN):  1547
MINIMIZATION ENDED:
DATE: (YR MO DAY):  80417 TIME (HR MIN):  1547
UNITS:  ENERGY IN GeV, DENSITY IN 1/fm^3
norm     960.2204+/-        298.4672 limits:      0.0100  4000.0000
temp       0.1650+/-          0.0056 limits:      0.1200     0.1800
lamq       1.1642+/-          0.0686 limits:      1.0000     1.9000
lams       1.0507+/-          0.0433 limits:      0.5000     1.9000
gamq  1.
gams  1.
lmi3       0.9857+/-          0.0204 limits:      0.5000     5.0000
lamc  1.
gamc  0.
dvol  0.
gam3  1.
```

[4] one line in the file

```
 CHEMICAL POTENTIALS:
 MU_B 0.0752  +/-0.0317  GeV
 MU_S 0.0169  +/-0.0159  GeV
 MUI3 -.0024  +/-0.0033  GeV

   TOP        BOTTOM        THEORY         EXP           ERROR        CHITERM    FEED-DOWN
tot_prime    prt_yield    501.364746      0.000000      0.000000      0.000000   WEAKnSTAR
totstrong    prt_yield    860.454234      0.000000      0.000000      0.000000   WEAKnSTAR
tot_multi    prt_yield    949.060683      0.000000      0.000000      0.000000   WEAKnSTAR
totenergy    totstrong      0.591791      0.000000      0.000000      0.000000   WEAKnSTAR
totenergy    tot_prime      1.015646      0.980000      0.010000      0.000000   WEAKnSTAR
netstrang    totstrang      0.003093      0.000000      0.050000      0.061864   WEAKnSTAR
netcharge    netbaryon      0.390004      0.390000      0.010000      0.000437   WEAKnSTAR
pi0139min    prt_yield    242.753922    237.000000     27.000000      0.213108   WEAKnSTAR
pi0139plu    prt_yield    235.145774    233.000000     26.000000      0.082530   WEAKnSTAR
Ka0492plu    prt_yield     36.224197     38.000000      8.100000     -0.219235   WEAKnSTAR
Ka0492min    prt_yield     31.098108     32.600000      6.900000     -0.217665   WEAKnSTAR
Lm1115zer    prt_yield     14.471336     13.880000      1.620000      0.365022   WEAKnSTAR
Lm1115zrb    prt_yield      7.612339      7.250000      0.855000      0.423788   WEAKnSTAR
Xi1321min    prt_yield      1.580377      1.840000      0.290000     -0.895252   WEAKnSTAR
Xi1321mnb    prt_yield      0.954049      1.160000      0.190000     -1.083951   WEAKnSTAR
UM1672min    prt_yield      0.251640      0.229000      0.073000      0.310134   WEAKnSTAR
UM1672mnb    prt_yield      0.187044      0.176000      0.037000      0.298488   WEAKnSTAR
pr0938plu    prt_yield     26.497716     34.300000      7.230000      0.000000   WEAKnSTAR
pr0938plb    prt_yield     11.487570     13.800000      2.980000      0.000000   WEAKnSTAR
pi0135zer    prt_yield    268.062350      0.000000      0.000000      0.000000   WEAKnSTAR
Ka0492sht    prt_yield     32.503232      0.000000      0.000000      0.000000   WEAKnSTAR
ph1020zer    prt_yield      4.659878      0.000000      0.000000      0.000000   WEAKnSTAR
Ka0892sht    prt_yield     10.431342      0.000000      0.000000      0.000000   WEAKnSTAR
Ka0892zer    prt_yield     11.508192      0.000000      0.000000      0.000000   WEAKnSTAR
....

....
totenergy    netbaryon     14.393940      0.000000      0.000000      0.000000   WEAKnSTAR
stranghad    netbaryon      2.555651      0.000000      0.000000      0.000000   WEAKnSTAR
entropy_t    netbaryon    100.703929      0.000000      0.000000      0.000000   WEAKnSTAR
pressuret    prdensity  0.845208E-01  0.820000E-01  0.500000E-02  0.000000E+00   WEAKnSTAR
prdensity    prt_yield    960.220423      0.000000      0.000000      0.000000   WEAKnSTAR
pressuret    prt_yield     81.158577      0.000000      0.000000      0.000000   WEAKnSTAR
netbaryon    prt_yield     35.376619     37.750000      0.700000      0.000000   WEAKnSTAR
entropy_t    prt_yield   3562.564524      0.000000      0.000000      0.000000   WEAKnSTAR
stranghad    prt_yield     90.410299      0.000000      0.000000      0.000000   WEAKnSTAR
totenergy    prt_yield    509.208919      0.000000      0.000000      0.000000   WEAKnSTAR
stranghad    prt_yield     90.410299      0.000000      0.000000      0.000000   WEAKnSTAR
totbaryon    prt_yield     91.301567      0.000000      0.000000      0.000000   WEAKnSTAR
totstrong    prt_yield    860.454234      0.000000      0.000000      0.000000   WEAKnSTAR
totenergy    totstrong      0.591791      0.000000      0.000000      0.000000   WEAKnSTAR
totstrang    prt_yield    180.263011      0.000000      0.000000      0.000000   WEAKnSTAR
tot_multi    prt_yield    949.060683      0.000000      0.000000      0.000000   WEAKnSTAR
 DATA POINTS: 12 PARAMETERS: 5 DoF: 7
 TOTAL CHI**2/DEG. OF FREEDOM  0.375148353
  SIGNIFICANCE OF FIT:   0.917311072
 [ (S-SBAR)/(S+SBAR) ]   0.00309318899
```

Figure 3.4: A typical `fitratios.out` file

CALC PLOT_DATA <3 13-letter filenames>

Generates three files which are optimized to be graphed by a package such as PAW, Mongo, Xmgrace or GNUPlot. The first file has a numerical list of ratios which were fitted, the second, a numerical list of calculated, but not fitted, ratios. The third has the experimental data, including the error bars.

CALC CHIPROFIL <12-letter file> tag L H P

This computes a χ^2/N_{DoF} profile of the Parameter designated by tag <Parameter tag> (see the thermal input file for a list), from the L to the H limit (real numbers), with P specifying the number of computed points (integer). The given file will store the main result, as a 2 column

table of the parameter value and χ^2/N_{DoF}. The minimum of each of the other parameters for each data point will also be stored in files in which the parameter is appended to the name. For instance, if the T, χ^2/N_{DoF} profile is stored in file 'prof_G_00-05' the minimal points of γ_q across the χ^2/N_{DoF} profile are stored in file 'prof_G_00-05_gamq'.

CALC SIGPROFIL This command is very similar to CALC CHIPROFIL. However, instead of the χ^2, the profile for the statistical significance is calculated. The command syntax is identical to CALC CHIPROFIL

CALC CHI2_CONT <9-letter filename> deviation tag1 tag2 Computes a $\chi^2/\mathrm{N_{DoF}}$ contour of parameters denoted by tag1 and tag2, with a given deviation from the χ^2/DoF minimum (*e.g.,* 1.1 for a $1.1 \times \chi^2_{\mathrm{min}}$ contour). The contour is stored in an output file 9 characters long.

Run log file `sharerun.out`

The complete 'log' for each run is saved in the file sharerun.out. This filename cannot be set by the user and the program overwrites it everytime it runs. This includes:

- The content of each input file (in the same format as read)
- A list of performed operations
- The output from MINUIT
- The content of each output file (in the same format as in the file)

If the program ends without a problem, the message 'PROGRAM TERMINATED SUCCESSFULLY' is printed, both on the screen and this file. If an error occurs, the program writes to the screen that an error has occurred, and outputs the details of the error to sharerun.out. The error can be tracked back from the last lines of the sharerun.out file, as there is the last operation that SHARE performed.

3.3 SHARE version 2

This is the up–to–date release of SHARE which is available online and which I used for fitting data from Au–Au collisions at $\sqrt{s_{NN}} = 62.4\,GeV$ (see the next section – section 4).

New features in SHAREv2

There are several things, which were updated in SHARE. At first, let us briefly go through them:
Fluctuations: In addition to particle yields, ratios and bulk quantities SHAREv2 can calculate, fit and analyze statistical fluctuations of particle yields and of particle ratios.

Decays: SHAREv2 has the flexibility to account for any experimental method of allowing for decay feed–downs to the particle yields, the weak feed–down input has been changed in order to make it easier for the user to introduce weak decay corrections.

Charm flavor: Charmed particles have been added to the decay tree, allowing as an option study of statistical hadronization of J/ψ, χ_c, D_c, etc.

Quark chemistry: Chemical non-equilibrium yields for both u and d flavors, as opposed to generically light quarks q, are considered; η–η' mixing, etc., are properly dealt with, and chemical non-equilibrium can be studied for each flavor separately;

Misc: Many new commands and features have been introduced and added to the basic user interface from SHAREv1. For example, it is possible to study combinations of particles and their ratios. It is also possible to combine all the input files into one file.

Other than that, SHAREv2 is backwards compatible, so all main features available in SHAREv1 (as described in previous section 3.2) works the same way as in SHAREv1.

3.3.1 Implementation of particle fluctuations

In grand–canonical ensemble, the particle yields and fluctuations can be calculated the following way. For a particle wih an energy $E_p = \sqrt{p^2 + m_i^2}$, the energy state occupancy is

$$n_i(E_p) = \frac{1}{\Upsilon_i^{-1} e^{E_p/T} \pm 1}, \tag{3.8}$$

where the upper sign is for ferimons, lower sign is for bosons. The Υ_i is the chemical fugacity as defined in eq. (2.72). Remind, that the yield average is obtained by multiplying the occupancy number (eq. 3.8) by the density of states (where V is volume and g degeneracy)

$$\langle N_i \rangle = gV \int \frac{d^3p}{(2\pi)^3} n_i(E_p). \tag{3.9}$$

The fluctuation in this number is then found to be:

$$\langle (\Delta N_i)^2 \rangle = \Upsilon_i \left. \frac{\partial \langle N_i \rangle}{\partial \Upsilon_i} \right|_{T,V} = gV \int \frac{d^3p}{(2\pi)^3} n_i(E_p)(1 \mp n_i(E_p)). \tag{3.10}$$

This can be evaluated to any desired accuracy by a conversion into an expansion of Bessel function terms in the following way:

$$\langle N_i \rangle = \frac{gVT^3}{2\pi^2} \sum_{n=1}^{\infty} \frac{(\pm 1)^{n-1} \Upsilon_i^n}{n^3} W\left(\frac{nm_i}{T}\right), \tag{3.11}$$

$$\langle (\Delta N_i)^2 \rangle = \frac{gVT^3}{2\pi^2} \sum_{n=1}^{\infty} \frac{(\pm 1)^{n-1} \Upsilon_i^n}{n^3} \binom{2+n-1}{n} W\left(\frac{nm_i}{T}\right), \tag{3.12}$$

where $W(x) = x^2 K_2(x)$. We assume the same convergence condition as for eq. (3.3), i.e $\Upsilon_i e^{-m_i/T} < 1$.

The eq. 3.12 neglects volume fluctuations, coming from centrality cuts and dynamics of system expansion. These are accounted for by dividing the observed fluctuation into an extensive and an intensive part,

$$\langle (\Delta X)^2 \rangle \approx \langle (\Delta x)^2 \rangle \langle V \rangle^2 + \langle x \rangle^2 \langle (\Delta V)^2 \rangle, \tag{3.13}$$

$\langle x \rangle$ and $\langle x^2 \rangle$ can be calculated by statistical method described in [7]. In case of particle ratio N_1/N_2, the fluctuations can be calculated as

$$\sigma^2_{N_1/N_2} = \frac{\langle (\Delta N_1)^2 \rangle}{\langle N_1 \rangle^2} + \frac{\langle (\Delta N_2)^2 \rangle}{\langle N_2 \rangle^2} - 2\frac{\langle \Delta N_1 \Delta N_2 \rangle}{\langle N_1 \rangle \langle N_2 \rangle}. \tag{3.14}$$

The last correlation term is given by the resonance decay into both particles

$$\langle \Delta N_1 \Delta N_2 \rangle = \langle N_1 N_2 \rangle - \langle N_1 \rangle \langle N_2 \rangle \simeq \sum_j B_{j \to 1,2} \langle N_j \rangle, \tag{3.15}$$

where $B_{j \to 1,2}$ is the branching ratio of j to decay into particle 1 or 2. Needless to say that ratio fluctuations does not depend on the system volume, since it cancels out from the numerator and denominator. For more information about particle fluctuations see [7] and references therein.

Experimental event–by–event fluctuations data points can be introduced to SHARE similarily as the particle yields an ratios into the `totratios.data` file (as described in section 3.2). The keyword for particle yield fluctuations is **fluct_yld**. So the input line should be in the following format:
particle1 fluct_yld data stat.err. syst.err. fit(0/1)
There are two more options for alternative definitions of fluctuations which are used for presentation of experimentaly measured fluctuations. They are implemented in SHAREv2, details can be found again in [7].

3.3.2 Decay feed–down and particle yields

As shown in [6, 7], decay feed–down is a fundamental component of the statistical hadronization model. However, the limited coverage of most detectors means that the feed–down coefficients will acquire an experimental correction, corresponding to the probability, that the decay products of a given resonance formed in the acceptance of the detector will stay there. These corrections need to be applied to both particle yields and fluctuations.

Weak decays such as $\Lambda \to p\pi^-$ are particularly susceptible to experimental acceptance as they happen in a macroscopic distance from the primary vertex. The weak decay feed–down correction include a geometrical as well as a momentum space component. Since the parent particles are not always observed directly, SHARE is capable to compute the final hadron multiplicities including experimental feed–down coefficients for all decays where the effect is not negligible.

In fact SHAREv2 present a sixth (optional) input file, which contains weak feed–down corrections. It is implemented to be included as a special line into the experimental data file `totratios.data`:
weakdecay file.feed
where 'weakdecay' is a keyword and 'file.feed' is the (9-letter) name of a file containing weak decay feed–down corrections. These will be applied to all following particle yields in the experimental data file until next 'weakdecay' statement.

Even though multiple feed–down files can be used in the same analysis, usually these files are experiment–specific. This way they can be easily kept track of. The feed–down file structure is the following for two–body (resp. three–body) decay:

Parent Daughter$_1$ Daughter$_2$ (Daughter$_3$) all/1st/2nd(/3rd)/cor coeff

The switch **all/1st/2nd(/3rd)** refers to what daughter parthicle the **coeff**icient applies. The **cor** switch refers to the fractional contribution of the acceptance to the two particle correlation $\langle \text{Daughter}_1\ \text{Daughter}_2 \rangle$ induced by a common resonance decay from parent. Here an example of a weak feed–down file is given in fig. 3.5 and an exemple of implementation in the experimental file in fig. 3.2.

```
#------------- Kaon feed-down
  #V1.X K_SL -> 2 PI   0.
Ka0492zer   pi0139plu   pi0139min   all   1.0000
  #V1.X WEAK K_S -> 2 PI   1.
Ka0492zer   pi0135zer   pi0135zer   all   1.0000
  #V1.X WEAK K_S -> 2 PI   1.
Ka0492zrb   pi0139plu   pi0139min   all   1.0000
  #V1.X WEAK K_S -> 2 PI   1.
Ka0492zrb   pi0135zer   pi0135zer   all   1.0000
  #V1.X K_L -> 3 PI   0.1
Ka0492zer   pi0139plu   pi0139min   pi0135zer   all      0.1000
  #V1.X K_L -> 3 PI   0.1
Ka0492zer   pi0135zer   pi0135zer   pi0135zer   all      0.1000
  #V1.X K_L -> 3 PI   0.1
Ka0492zer   pi0139plu   el0000min   nue000zer   all      0.1000
  #V1.X K_L -> 3 PI   0.1
Ka0492zer   pi0139min   el0000plu   nue000zer   all      0.1000
  #V1.X K_L -> 3 PI   0.1
Ka0492zer   pi0139plu   mu0000min   num000zer   all      0.1000
Ka0492zer   pi0139min   mu0000plu   num000zer   all      0.1000
  #V1.X K_L -> 3 PI   0.1
Ka0492zrb   pi0139plu   pi0139min   pi0135zer   all      0.1000
  #V1.X K_L -> 3 PI   0.1
Ka0492zrb   pi0135zer   pi0135zer   pi0135zer   all      0.1000
  #V1.X K_L -> 3 PI   0.1
Ka0492zrb   pi0139plu   el0000min   nue000zer   all      0.1000
  #V1.X K_L -> 3 PI   0.1
Ka0492zrb   pi0139min   el0000plu   nue000zer   all      0.1000
  #V1.X K_L -> 3 PI   0.1
Ka0492zrb   pi0139plu   mu0000min   num000zer   all      0.1000
Ka0492zrb   pi0139min   mu0000plu   num000zer   all      0.1000
```

Figure 3.5: An exemple of a weak decay feed–down input file.

There are two special cases where no feed–down file is needed. These are: **weakdecay UNCORRECT**, which means, that all weak decays contributions to particle yields are fully accepted by SHARE. The other extremity is **weakdecay NOWK_FEED**, which means, that all experimental particle yields

are without the contributions from weak decays of resonances. This case, from the perspective of experimental data, means that either all weak decay products are not accepted and/or have been all corrected for in experimental yields by the offline analysis groups.

For the implementation of other features, the reader is refered to [6, 7], where a full description is given.

4 Au–Au collisions at $\sqrt{s_{NN}} = 62.4\,\mathrm{GeV}$

My study was concentrated on the centrality dependence of thermal parameters of statistical hadronization model as they are defined in SHAREv2 in Au–Au collisions at $\sqrt{s_{NN}} = 62.4\,\mathrm{GeV}$. First of all, I had to collect data (mostly from RHIC) and prepare them for analysis.

4.1 Input data

As sources I used [10] for non-strange particle yields, [11] for strange particle yields and [12] for Λ and $\overline{\Lambda}$ yields. First, the centrality bins from the sources needed to be unified. Therefore I fitted the yields of each particle across centrality with a function in the form

$$f(x) = a \cdot e^{bx} \left(1 - x\right)^c , \tag{4.1}$$

where a, b, c are real constants and x is the centrality in %, where 0% counts as a head–on collision and 100% as a miss. The largest centrality bin (for most peripheral collisions) used in the analysis is $(70 - 80)\%$. A summary of data available is in appendix A. To fill in all the centrality bins, I fitted each particle species separately and the result can be seen in fig.4.1.

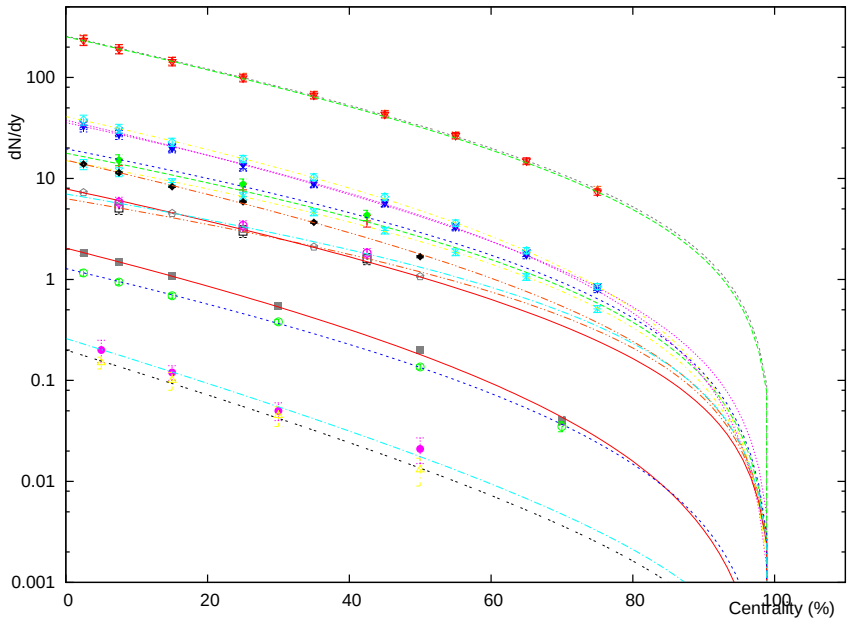

Figure 4.1: Particle yields fitted across centrality. Points correspond to the experimental data. From the top: πs, Ks, p, $\overline{p}$, Λs, Ξs, and Ωs

The centrality expressed in % can be easily transformed into number of participants by a fit of number of participants with a function

$$f(x) = a \cdot e^{bx} + c \tag{4.2}$$

where again a, b, c are real fit parameters and x the centrality in %. As can be seen in figure 4.2, it describes the data (available from [13]) very nicely.

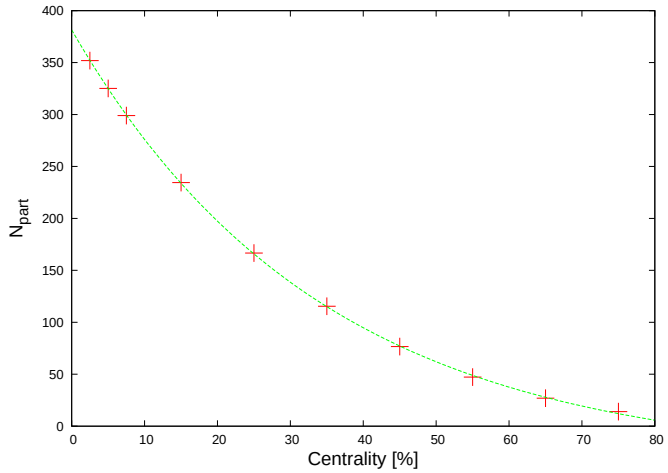

Figure 4.2: Number of participants in a collision vs. centrality with fit by $f(x) = a \cdot e^{bx} + c$.

Further on, I will present my results dependent on the centrality in %. The final fits, on which I base my further results, have the statistical significance ranging from 97.69% (which corresponds to $\chi^2/N_{DoF} \approx 0.235$) for the most central collision in non-equilibrium model to 2.26% (which corresponds to $\chi^2/N_{DoF} \approx 2.27$) for the most peripheral collision in the equilibrium model. Generally, the peripheral collisions lacks significance due to bad statistics and large errors in the experimental data. Also one should note, that non–equilibrium model has two more free parameters to fit than the equilibrium model and therefore its χ^2/N_{DoF} is normally lower and the fit (from mathematical point of view) better. To have a better idea of how good the fits are, the statistical significances are summarized in table 4.1.

4.2 Centrality dependence of statistical parameters

First of all, let us have a look at the evolution of the chemical freeze–out temperature across centrality in all three, equilibrium, semi-equilibrium and non-equilibrium models. Each of the centrality bins was fitted separately and independently from each other. After that, the results from each fit from SHARE are plotted and fitted with GNUPlot with a linear function, if not said otherwise. The temperature centrality dependence can be seen in figure 4.3. The other observable, which is of interest is the baryo–chemical potential μ_B. Its centrality dependence can be seen in figure 4.4. Now let us discuss the main differences between the models. It is clearly visible from the plots, that as soon as chemical equilibrium for strangeness is released, the temperature T changes its behavior; it decreases with centrality going from central to peripheral collisions. The baryo–chemical potential μ_B keeps its tendency to slowly decrease from central to peripheral collisions. Because λ_s stays almost constant for all three models (it is a free parameter in all fits), this difference is that in semi–

Centrality [%]	equilibrium	semi–equilibrium	non-equilibrium
0-5	91.7%	89.6%	97.7%
0-10	88.2%	81.4%	92.8%
5-10	83.4%	78.1%	91.1%
10-20	81.9%	72.4%	82.8%
20-30	81.7%	73.9%	75.6%
20-40	32.0%	31.4%	38.6%
30-40	24.4%	19.4%	25.6%
40-50	85.3%	84.8%	83.8%
40-60	40.8%	48.0%	58.1%
50-60	43.4%	83.6%	67.2%
60-70	60.6%	98.2%	85.1%
60-80	14.2%	84.4%	76.7%
70-80	2.6%	99.4%	70.9%

Table 4.1: Table of statistical significances of the fits used for analysis

and non–equilibrium model, the phase space occupancy γ_s is released and fitted. The phase space occupancy of strangeness is approaching the value of 2 for the most central collisions.

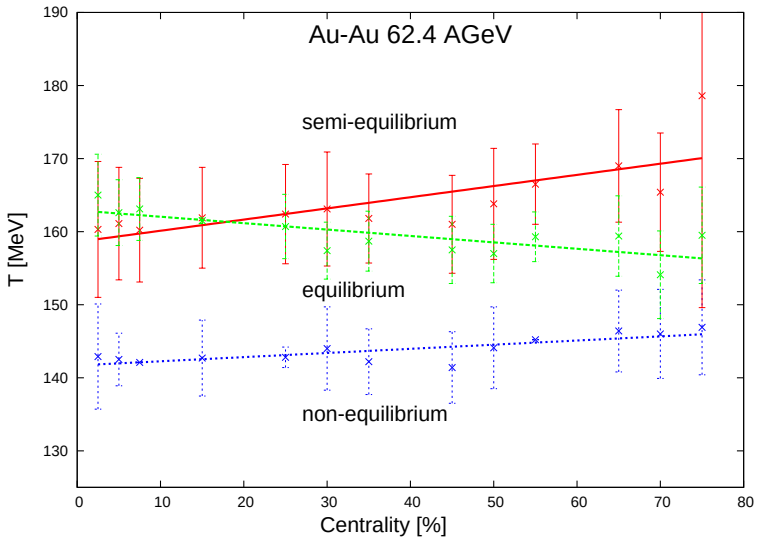

Figure 4.3: Chemical freeze–out temperature vs. centrality of three statistical models fitted with a linear functions.

Since there is no major difference bettween the γ_s and γ_q, the γ_q is released and fitted as well. Usually the dependence of strangeness phase space occupancy is normalized to light quark phase space occupancy γ_q. Their ratio γ_s/γ_q across centrality is shown on figure 4.5 for the semi– and non–equilibrium models. For equilibrium the ratio is equal to 1 by definition.

One can see that the ratio γ_s/γ_q holds the same pattern across centrality, it falls with centrality. For most central collisions, the strnageness is enhanced

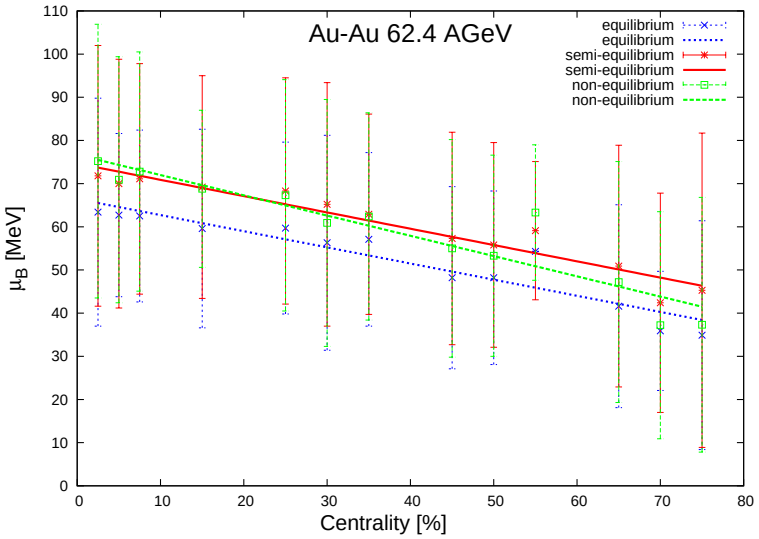

Figure 4.4: Baryo–chemical potential vs. centrality of three statistical models fitted with a linear functions.

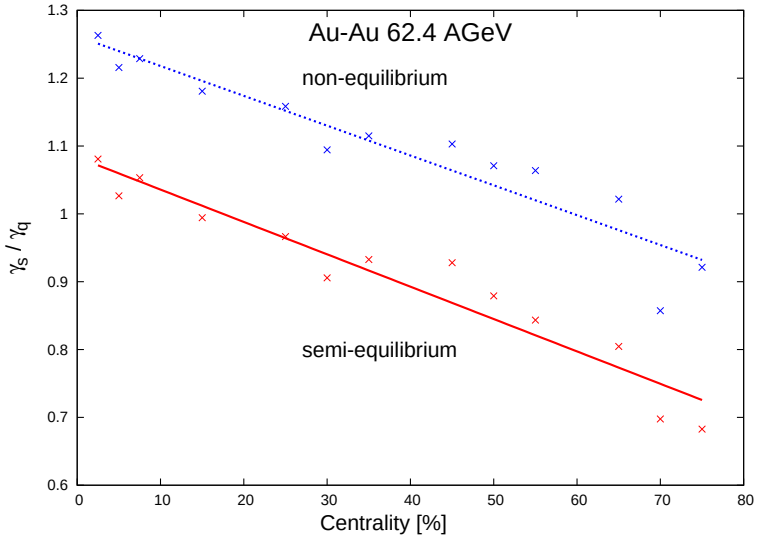

Figure 4.5: Evolution of γ_s/γ_q across centrality for the non-equilibrium and semi-equilibrium model.

with respect to light quark abundance in both semi– and non–equilibrium models. On the other hand, for peripheral collisions, the strangeness production is suppressed. It is in accordance with the temeperature evolution as seen in fig. 4.3.

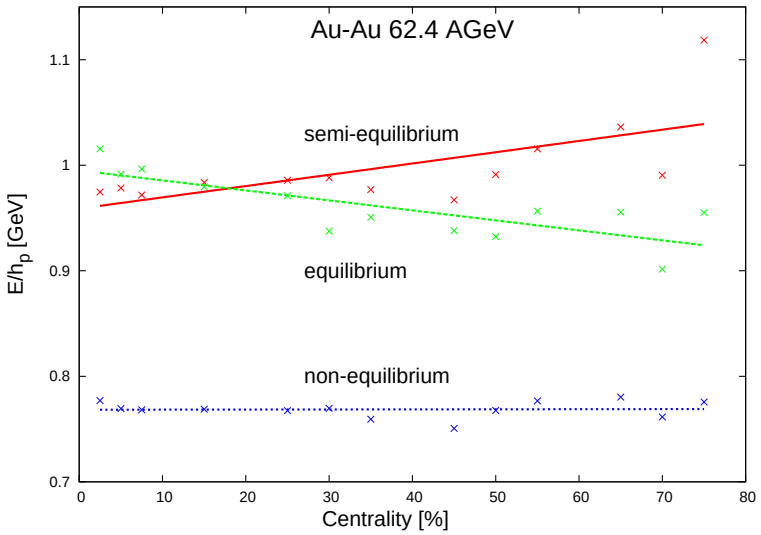

Figure 4.6: Energy per primary hadron across centrality

4.3 Hadronization conditions

During my analysis, I have come across several hadronization conditions, which needed to fulfilled (consulted with [13]). To make the fits 'fall' into a physical χ^2 minimum, apart from experimental data I have fitted the strangeness conservation in the following form:

$$\frac{< s > - < \overline{s} >}{< s > + < \overline{s} >} \rightarrow 0.00 \pm 0.05. \tag{4.3}$$

Another constraint applied for the non–equilibrium fit is

$$\frac{E}{TS} > 1 \qquad \text{i.e.} \quad \frac{E}{TS} \rightarrow 1.02 \pm 0.015, \tag{4.4}$$

for the system to explode. But the most interesting thing I came across during the fitting procedure was, that the energy per primary hadron E/h_p stays constant across whole centrality very precisely for non–equilibrium and remains constant within the error for semi–equilibrium and equilibrium fits too (see figure 4.6). Again, the different behavior of equilibrium model is caused by fixed $\gamma_s = 1$. It should hold for all centralities at $E/h_p \approx 0.77$ for $\gamma_q \sim 1.6$ fitted, and $E/h_p \approx 0.98$ for $\gamma_q = 1$ fixed.

According to [13], there is a complementary hadronization condition, which is the pressure. We have identified $P = 82\,\mathrm{MeV/fm^3}$; pressure has properties of a density and does not see the volume. Each of these constraints turned out not to be enough itself, but their combination seem to be a good sign of hadronization.

5 Conclusion and outlook

In this thesis, we have presented the statistical hadronization model and its implementation in the SHARE program package. After I explored the vast possibilities of the program, I fitted data from Au–Au collisions at $\sqrt{s_{\mathrm{NN}}} = 62.4\,\mathrm{GeV}$ from RHIC. Other data was succesfully fitted by others within the SHM framework using SHARE (e.g. Au–Au at $\sqrt{s_{\mathrm{NN}}} = 200\,\mathrm{GeV}$ from RHIC [14]).

Having done the fitting of particle yields, I concentrated myself on the differences between the three models of chemical *equilibrium*, where the light quark as well as strangeness phase space occupancy is fixed to 1 ($\gamma_q = 1,\ \gamma_s = 1$), *semi–equilibrium*, which comprises the release of strangeness phase space occupancy ($\gamma_q = 1,\ \gamma_s \neq 1$), and *non–equilibrium*, where both phase space occupancies are released and being fitted ($\gamma_q \neq 1,\ \gamma_s \neq 1$). The light quark phase space occupancy γ_q remains almost constant in the non–equilibrium model, but the value of $\gamma_q \approx 1.58$ seems to describe best the data. On the other hand, there is a clear evolution of the strangeness phase space occupancy γ_s across centrality. In most central collisions, there appears to be more strangeness produced, the phase space is over–saturated. But in the most peripheral collisions, the γ_s decreases below 1, the strangeness phase space is undersaturated (see figure 4.5)

Further, there appears to be a combination of hadronization conditions, which applies for the non–equilibrium model across all centralities and that is pressure $P = 82\,\mathrm{MeV/fm^3}$ and energy per primary hadron $E/h_p \approx 0.77$. The energy per primary hadron work also for semi– and equilibrium models, but has a different value, because of different value of γ_q.

It appears that the non–equilibrium model describes best the data. If we have a look at temperature vs. centrality (figure 4.3), it seems that the temperature is constant across centrality in all the models. This fact leads to an upgrade to SHARE to be able to fit multiple datafiles at the same time with shared parameter(s), temperature T in this case. Assuming that the temperature is really constant for all centralities, this would bring far more better results, because of the ratio of free parameters and datapoints to be fitted. Work on so called SHAREv3 (which will be capable of doing this) is already in progress, unfortunetelly not far enough to give any new results other than SHAREv2 would give. Backward compatibility is maintained as much as possible. I plan to work on this in the future to confirm the results not only presented in this thesis but for other energies and different collisional systems as well.

References

[1] Jean Letessier and Johann Rafelski, 2002, Hadrons and Quark-Gluon Plasma, *Cambridge University Press*

[2] Giorgio Torrieri, 2004, STATISTICAL HADRONIZATION PHENOMENOLOGY IN HEAVY ION COLLISIONS AT SPS AND RHIC ENERGIES (PhD.Thesis), *http://arXiv.org/abs/nucl-th/0405026v2*

[3] Hagiwara, K. and others, 2002, Review of Particle Physics, *Physical Review D***66**

[4] F.Cooper, G.Frye, 1974, Single-particle distribution in the hydrodynamic and statistical thermodynamic models of multiparticle production, *Physical Review D***10**

[5] J.Rafelski, 2008, Strangeness enhancement, *Eur. Phys. J. Special Topics* **155**

[6] G. Torrieri, S. Steinke, W. Broniowski, W. Florkowski, J. Letessier, and J. Rafelski, 2004, SHARE: Statistical Hadronization with Resonances, *arXiv:nucl-th/0404083v2*

[7] G. Torrieri, S.Jeon, J.Letessier,J.Rafelski, 2007, SHAREv2: fluctuations and comprehensive treatment of decay feed–down, *arXiv:nucl-th/0603026v2*

[8] F. James, 1994, MINUIT – Function Minimization and Error Analysis, *CERN Program Library entry D506*

[9] J.Letessier, J.Rafelski, 2005, Centrality dependence of strangeness and (anti)hyperon production at BNL RHIC, *arXiv:nucl-th/0506044v2*

[10] L.Molnár, 2006, SYSTEMATICS OF IDENTIFIED PARTICLE PRODUCTION IN pp, dAu AND Au-Au COLLISIONS AT RHIC ENERGIES, PhD Thesis, *STAR collaboration, http://drupal.star.bnl.gov/STAR/files/startheses/2006/molnar_levente.pdf*

[11] J.Speltz, 2006, Characterisation of a dense state of quarks and gluons by the multi–strange hyperons excitation functions as measured with the STAR experiment at RHIC, PhD Thesis *STAR collaboration, http://drupal.star.bnl.gov/STAR/files/startheses/2006/speltz_jeff.pdf*

[12] Personal communication with Jun Takahashi.

[13] Personal communication with Johann Rafelski and Jean Letessier.

[14] G.Torrieri, S.Jeon, J.Rafelski, 2005, A statistical model analysis of yields and fluctuations in 200 GeV Au–Au collisions, *arXiv:nucl-th/0509067v1*

A Appendix

In this appendix one can find the important data sources that I used for my analysis.

System	Centrality	π^-	π^+	K^-	K^+	$\bar{p}$	p
	min-bias	1.46 ± 0.10	1.44 ± 0.10	0.15 ± 0.01	0.15 ± 0.01	0.10 ± 0.01	0.11 ± 0.01
	bin 1	0.33 ± 0.02	0.35 ± 0.02	0.03 ± 0.01	0.03 ± 0.01	0.02 ± 0.01	0.03 ± 0.01
pp	bin 2	1.29 ± 0.09	1.31 ± 0.09	0.13 ± 0.01	0.13 ± 0.01	0.09 ± 0.01	0.10 ± 0.01
200 GeV	bin 3	2.23 ± 0.16	2.28 ± 0.16	0.23 ± 0.02	0.23 ± 0.03	0.16 ± 0.01	0.17 ± 0.01
	bin 4	3.10 ± 0.22	3.15 ± 0.23	0.32 ± 0.02	0.32 ± 0.02	0.22 ± 0.02	0.25 ± 0.02
	bin 5	4.28 ± 0.31	4.33 ± 0.31	0.44 ± 0.03	0.49 ± 0.04	0.32 ± 0.02	0.34 ± 0.02
	min-bias	4.65 ± 0.34	4.65 ± 0.34	0.58 ± 0.04	0.59 ± 0.04	0.42 ± 0.03	0.47 ± 0.04
d-Au	40 - 100%	2.89 ± 0.21	2.87 ± 0.22	0.32 ± 0.03	0.36 ± 0.03	0.24 ± 0.02	0.28 ± 0.03
200 GeV	20 - 40%	6.06 ± 0.45	6.01 ± 0.44	0.75 ± 0.05	0.81 ± 0.06	0.56 ± 0.04	0.65 ± 0.05
	0 - 20%	8.43 ± 0.62	8.49 ± 0.63	1.04 ± 0.07	1.19 ± 0.09	0.79 ± 0.06	0.93 ± 0.07
	70 - 80%	7.77 ± 0.57	7.35 ± 0.54	0.80 ± 0.06	0.85 ± 0.06	0.51 ± 0.04	0.84 ± 0.06
	60 - 70%	14.7 ± 1.1	14.9 ± 1.1	1.73 ± 0.13	1.93 ± 0.14	1.06 ± 0.08	1.82 ± 0.13
	50 - 60%	26.8 ± 2.1	26.6 ± 1.9	3.27 ± 0.24	3.61 ± 0.27	1.86 ± 0.14	3.36 ± 0.25
62.4 GeV	40 - 50%	43.8 ± 3.4	43.2 ± 3.4	5.64 ± 0.43	6.58 ± 0.50	3.05 ± 0.23	5.68 ± 0.43
	30 - 40%	67.5 ± 5.5	66.6 ± 5.4	8.78 ± 0.70	10.3 ± 0.8	4.64 ± 0.37	8.88 ± 0.70
Au - Au	20 - 30%	101 ± 9	98.9 ± 8.5	13.7 ± 1.2	15.6 ± 1.31	6.65 ± 0.65	12.9 ± 1.1
	10 - 20%	146 ± 13	144 ± 14	19.7 ± 1.8	22.9 ± 2.1	9.12 ± 0.83	20.2 ± 1.9
	5 - 10%	192 ± 20	191 ± 20	27.1 ± 2.8	31.2 ± 3.16	11.6 ± 1.2	28.8 ± 2.9
	0 - 5%	237 ± 27	233 ± 26	32.6 ± 3.7	38.0 ± 4.3	13.8 ± 1.6	34.3 ± 3.8

Figure 1.1: Integrated multiplicity density dN/dy of identified particles for various collision systems and centralities. Errors are the quadratic sum of statistical and systematic errors, but dominated by systematic errors (taken over from [10]).

centralité	Ξ^-	$\overline{\Xi}^+$	Ω^-	$\overline{\Omega}^+$
0 % - 5 %	1,84 ± 0,11	1,16 ± 0,08	0,20 ± 0,05	0,15 ± 0,02
5 % - 10 %	1,50 ± 0,08	0,94 ± 0,06		
10 % - 20 %	1,09 ± 0,07	0,69 ± 0,04	0,12 ± 0,02	0,10 ± 0,02
20 % - 40 %	0,55 ± 0,03	0,38 ± 0,02	0,050 ± 0,010	0,045 ± 0,010
40 % - 60 %	0,201 ± 0,009	0,136 ± 0,007	0,021 ± 0,06	013 ± 0,004
60 % - 80 %	0,040 ± 0,004	0,035 ± 0,004		

Figure 1.2: Multiplicity density dN/dy of $\Xi^-, \overline{\Xi}^+, \Omega^-, \overline{\Omega}^+$ for different centralities in Au–Au collisions at $\sqrt{s_{\mathrm{NN}}} = 62.4\,\mathrm{GeV}$. The errors are quadratic sums of systematic and statistical errors.